Trends in Food Science & Technology 111 (2021) 151–165

Contents lists available at ScienceDirect

Trends in Food Science & Technology

journal homepage: www.elsevier.com/locate/tifs

Rapid and noninvasive sensory analyses of food products by hyperspectral imaging: Recent application developments

Gözde Özdoğan, Xiaohui Lin, Da-Wen Sun *

Food Refrigeration and Computerized Food Technology (FRCFT), School of Biosystems and Food Engineering, Agriculture & Food Science Centre, University College Dublin (UCD), National University of Ireland, Belfield, Dublin 4, Ireland

ARTICLE INFO

Keywords:
Hyperspectral imaging technology
Sensory analysis
Texture
Colour
Flavour

ABSTRACT

Background: Sensory analysis is the evaluation of the signals received through senses of sight, sound, taste, smell, and touch. The traditional methods for the analysis of sensory properties including trained sensory panel, colourimeters and texture analysers are invasive, laborious, and small-scale procedures. Hyperspectral imaging systems (HSI) has emerged as a less time-consuming and non-destructive method to determine the sensory properties of a diverse range of food products.

Scope and approach: This review provides a comprehensive overview of recent application developments since 2010 for identifying sensory properties including colour, defects, texture, flavour, freshness, and maturity in various food products by HSI.

Key findings and conclusions: The Vis-NIR (400–1000 nm) hyperspectral imaging is most used for the assessment of sensory properties. Moreover, the commonly applied multivariate analysis in the sensory evaluation by HSI is linear regression algorithms (PLSR and MLR), but non-linear analysis achieves better performance for the prediction of sensory features. Regression models are applied for determining the texture, colour, flavour, and freshness of food products while classification models are used to detect the defects and maturity by which the most accurate results are obtained. Furthermore, the combination of algorithms and the integration of spectral and spatial information yield more accurate results in the assessment of sensory features. Although there are still some limitations to overcome for the improvement of the HSI system, studies on the application of HSI in the real-time monitoring of sensory properties have proved a great potential for industrial applications.

1. Introduction

The first impression of a food product by the consumer is the appearance, texture and taste, which are the basic sensory properties. Appearance includes optical properties (colour, gloss, and uniformity), physical shape features (size, shape and surface texture), and presentation form features (packaging, lighting and contrast) (Murray et al., 2001). Moreover, the texture is directed towards the senses perceived immediately after the appearance. It is divided into two groups as finger feeling (hardness, softness and juiciness) and mouth feeling (chewiness, gumminess, grainy, roughness and floury). Flavour is a combination of taste and smell perceptions. In addition to the perception of taste (sweet, salty, sour, bitter, metallic, and umami flavours), a sensation of warmth and bitterness is also possible. Besides these properties, physical, and mechanical defects can contribute to many sensory properties (Lawless & Heymann, 2013).

Nowadays, sensory assessment of food products attracts significant attention in the food industry since consumers prefer to buy foods that can guarantee the overall acceptability and satisfaction. As consumers are becoming particularly more deliberate about sensory properties such as colour, texture, and flavour, and the food industry needs to determine the overall acceptability of a food item and to define the sensory characteristics that are vital for the food, the need for the development of rapid and reliable sensory assessment methods is obvious.

Traditionally, sensory attributes of food products are evaluated by trained human panellists, however, trained panel evaluation is subjective, and not suitable for immediate application when needed. Instrumental methods are also available, including texture profile analysis for textural characteristics (Szczesniak, 2002), chromameters for colour features (MacDougall, 2010), GC-O-MS for flavour compounds (Song & Liu, 2018),

* Corresponding author.
E-mail address: dawen.sun@ucd.ie (D.-W. Sun).
URL: http://www.ucd.ie/refrig, http://www.ucd.ie/sun (D.-W. Sun).

https://doi.org/10.1016/j.tifs.2021.02.044
Received 30 October 2020; Received in revised form 25 January 2021; Accepted 19 February 2021
Available online 25 February 2021

but these methods are still time-consuming, small-scale, and destructive. On the other hand, various imaging and spectroscopic technologies have emerged as alternative tools for the food industry, particularly, in recent years, hyperspectral imaging technology has gained significant importance as a rapid and noninvasive method for detecting large-scale samples (Liu et al., 2017). Therefore, several reviews of the application of HSI have been published, covering the prediction of the textural properties (Lei & Sun, 2019; Ma et al., 2019; Wang et al., 2016; Xiong et al., 2014) and colour features (ElMasry, Sun, & Allen, 2012; ElMasry & Nakauchi, 2016; Wu & Sun, 2013b) of food products. However, no review is available focusing on a wide range of the sensory properties of food products evaluated by HSI.

Therefore, the current review aims to provide comprehensive information since 2010 on the implementation of hyperspectral imaging technology in the evaluation of the sensory features of food products. In the review, hyperspectral imaging technology is briefly introduced, key steps of image processing and application developments in evaluating colour, defects, texture, flavour, freshness, and maturity are discussed. In addition, the advantages and the challenges of the HSI technology are presented and perspectives in future studies are also highlighted.

2. Fundamentals of hyperspectral imaging technology

Hyperspectral imaging systems integrate imaging and spectroscopy to obtain spatial and spectral data in one system. A hyperspectral imaging system produces three dimensional (3-D) hypercubes including two-dimensional spatial data and one-dimension spectral data, forming a stack of images at continuous wavelengths, and every image at a specific wavelength is called sub-image (see Fig. 1b and c) and can be defined as I (x, y, λ), i.e., a spatial image I (x, y) at different wavelengths (λ) (Kamruzzaman et al., 2013; Xiong et al., 2014).

Hypercubes are commonly obtained in three sensing modes of reflectance, transmittance, and interactance (Wu & Sun, 2013a). The reflectance mode is generally used for the evaluation of external quality properties such as size, surface texture, and physical defects, while the transmittance mode is often employed for evaluating compositions or internal defects. In addition, for obtaining deeper information about food products, the interactance mode can be utilized. Thus, it is important to select the most convenient acquisition mode according to the purpose of analysis and the properties of food products.

For HSI image acquisition, there are four different approaches available, including point scanning (whisk-broom), line scanning (push-broom), area scanning, and the single shoot procedure. Among these methods, line scanning is the most used tool in the food industry, since it can scan continuously in one direction, and thus suitable for conveyor belt systems (ElMasry & Nakauchi, 2016).

Basically, a hyperspectral system consists of a computer with proper software, a spectrograph, a camera, and an illumination unit (Sun, 2010). An example diagram of the system is shown in Fig. 1a. Various procedures are performed to both protect necessary data and to reduce redundant information and the dimensionality of the data since hypercubes have a considerable number of data. There are three main steps in

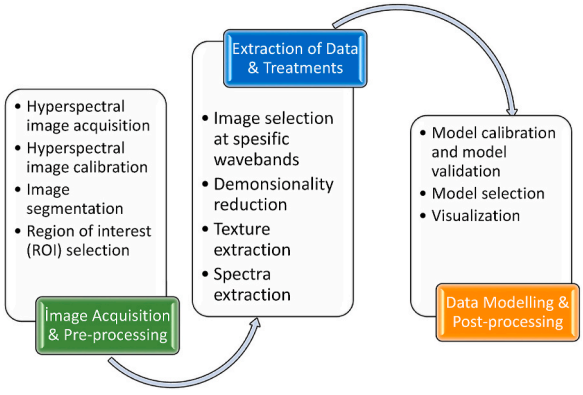

Fig. 2. General steps of hyperspectral imaging process.

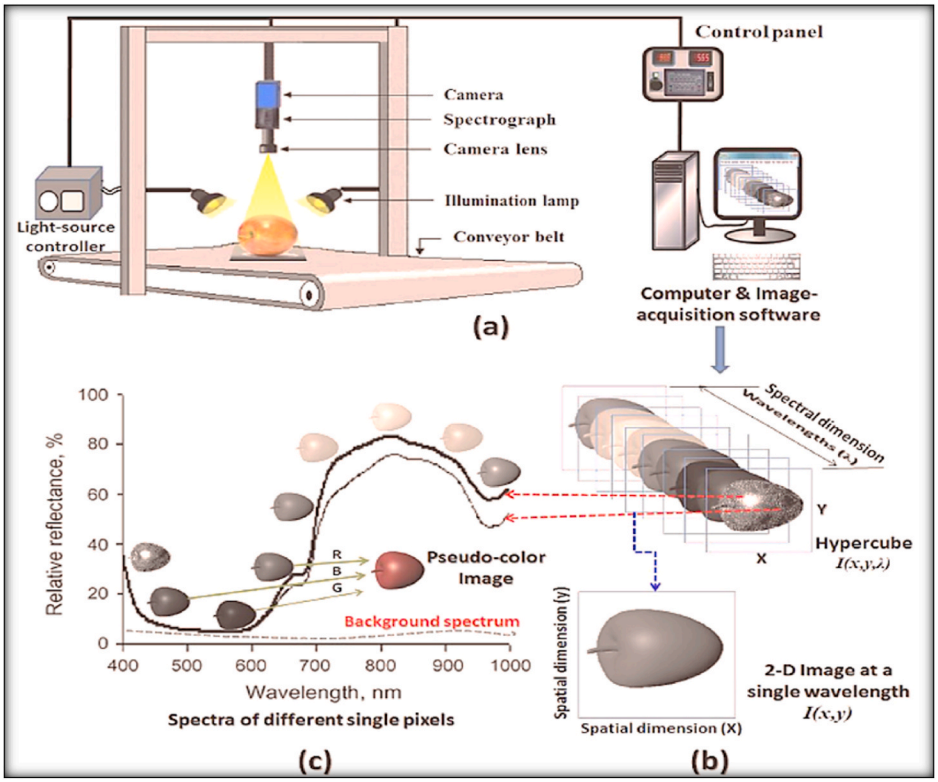

Fig. 1. (a) A schematic diagram of hyperspectral imaging (b) an example of 2-D sub-images (c) spectra of any pixels in the hypercube (ElMasry & Nakauchi, 2016).

the processing of hypercubes: image acquisition and pre-processing, extraction of data and treatments, data modelling and post-processing (Fig. 2).

In the first step, the instrumental setups such as sensing mode, type of detector and exposure time are adjusted. The wavelength calibration and image acquisition are also completed in this stage. Additionally, there is a need for a mandatory step called unfolding, which is about reducing the 3-D form of hypercubes to a 2-D data matrix since chemometrics can be applied to process the 2-D information (Cheng et al., 2017b). Many spectral pre-treatments including normalization, filtering, smoothing, standard normal variate (SNV), Fourier transform (FT), multiplicative scatter correction (MSC), the Savitzky–Golay (SG) are used to reduce noises and remove redundant information (Pan et al., 2018). Moreover, selecting the region of interests (ROIs) are performed for image segmentation using some algorithms such as thresholding, and edge-based segmentation (Ma et al., 2019). In order to create data modelling for classification or regression, numerous multivariate analysis, including principal component analysis (PCA), multi-linear regression (MLR), partial least squares regression (PLSR), partial least square discriminant analysis (PLS-DA), soft independent modelling of class analogy (SIMCA), Fishers discriminant analysis (FDA), support vector machine (SVM), artificial neural network (ANN) are generally implemented (Lin & Sun, 2020).

Furthermore, the coefficient of determination and the root mean square error for calibration (R^2_C, RMSEC), cross-validation (R^2_{CV}, RMSECV) and prediction (R^2_P, RMSEP) are used for assessment of the performances of models. For a model to be considered good in performance, it must have higher values of R^2 and lower values of error (Su & Sun, 2018).

In the applications of hyperspectral imaging, the evaluation of sensory features of food products is one of the main areas. The determination of sensory attributes of food products such as appearance (i.e., colour, shape, and physical defects) and textural properties (i.e., hardness, cohesiveness, and chewiness) are essential for identifying the needs of customers and providing preferable and satisfactory food products. Moreover, sensory attributes are important for the estimation of the quality of food products during food processing such as drying, freezing and cooking. Hence, the utilization of hyperspectral imaging systems as a sensory assessment method of food sensory quality attracts research attention.

HSI principally rely on chemometric analysis for evaluating food sensory quality attributes, and the relation between molecular bonds and wavebands are crucial to deeply understand the chemistry behind the models (Lin & Sun, 2020). Therefore, band assignments play a key role in identifying chemical constituents. Table 1 summarizes the band assignments in the sensory assessment of different food products by HSI since 2010.

Table 2 summarizes the applications of hyperspectral imaging technology in evaluating food sensory properties. The frequency (f) of studies on hyperspectral imaging technology for the evaluation of sensory features since 2010 is shown in Fig. 3. The order of the application frequency of sensory properties is texture (f = 42) > colour (f = 22) > defects (f = 20) > freshness (f = 18) > maturity (f = 16) > flavour (f = 15). On the other hand, the order of types of food products in the application of HSI for sensory evaluation is fruits (f = 56) > meat (f = 53) > other products (f = 15) > vegetables (f = 9). The hyperspectral imaging technology is mostly used for the prediction of texture in the food products, especially in fruits and meat. However, studies on the prediction of flavour, maturity and bruises have increased in recent years.

Table 1
Band assignments of HSI based on the literature.

Food Type	Wavelengths (nm)	Assignment	References
Meat and Meat Products	430	Hemoglobin	Kamruzzaman et al. (2016a,b)
	440	Deoxymyoglobin	Jiang et al. (2018)
	500	Astaxanthin	Dai et al. (2015)
	545	Oxymyoglobin	Wu, Peng, et al. (2012)
	575	Metmyoglobin	Wu, Peng, et al. (2012)
	635	Sulfmyoglobin	Wu, Peng, et al. (2012)
	780	O–H stretching third overtones	Kamruzzaman et al. (2016a,b)
	880	N–H out-of-plane bend of amine	Yang et al. (2017)
	900–940	C–H stretching third overtones	Cheng, Sun, Pu, Wang, and Chen (2015)
	970	O–H stretching second overtone	Kamruzzaman et al. (2012)
	1440	O–H stretching first overtone	Kamruzzaman et al. (2012)
	1211	C–H stretching second overtone	Kamruzzaman et al. (2012)
	1500	N–H stretching first overtone	ElMasry et al. (2011)
	1650–1680	C–H stretching first overtone	Barbin et al. (2012)
	1896	O–H stretching second overtone	Yang et al. (2018)
Fruits and Vegetables	435	Carotenoid	Huang et al. (2014)
	450	β-carotene	Munera et al. (2017)
	535	Anthocyanin	Huang et al. (2014)
	657–839	N–H stretching third overtone	Ye et al. (2018)
	660	Chlorophyll	Huang et al. (2014)
	678, 705	C–H stretching fourth overtone	Xiao et al. (2020)
	780	Lycopene	Roy et al. (2017)
	880–890	C–H stretching third overtone	Xiao et al. (2020)
	970	O–H stretching second overtone	Nguyen-Do-Trong et al. (2018)
	1190	C–H stretching second overtone	Rahman, Faqeerzada, and Cho (2018)
	1426–1489	O–H stretching first overtone	Esquerre et al. (2012)
	1370–1398	C–H combinations first overtone	Esquerre et al. (2012)
	1580–1700	C–H stretch first overtone	Ferrari et al. (2015)
	1600	Tannins	Rodríguez-Pulido et al. (2014)
Others (coffee beans)	1680, 2250, 2425	Caffeine	Caporaso et al. (2018)
	1668, 2269	Trigonelline	Caporaso et al. (2018)
	1460–1700	Sucrose	Caporaso et al. (2018)
	1430	C–H stretch and C–H deformation vibration	Caporaso et al. (2018)
	1730	C–H stretching third overtone	Caporaso et al. (2018)
	1760	C–H stretching second overtone	Caporaso et al. (2018)

3. Evaluation of visual sensory features of food products

3.1. Colour

As colour is the first feature noticed by consumers, it is one of the most vital sensory quality characteristics, which has a significant impact on the purchasing decision of consumers by indicating some information about the physical, chemical, or microbiological quality of food products. For instance, many consumers associate vivid and natural colour with superior quality and appeal, while an unexpected colour generally gives the opposite impression. Although there are instruments such as colourimeters giving X (red), Y (green) and Z (blue) and chromameters giving L^* (lightness), a^* (reddish - greenish) and b^* (bluish - yellowish) for colour evaluation, these devices can be problematical for colour assessment, especially when the sample is nonhomogeneous with

Table 2
Applications of hyperspectral imaging in the evaluation of the sensory properties of food products.

Products	Food Type	Sensory features	Wavelengths (nm)	Models	Accuracy	References
Beef	Meat	Tenderness (WBSF)	400–1100	MLR	$R^2_{CV} = 0.91$	Wu et al. (2012b)
		Colour (*L**)			$R^2_{CV} = 0.96$	
		Colour (*a**)			$R^2_{CV} = 0.96$	
		Colour (*b**)			$R^2_{CV} = 0.97$	
		Tenderness (SSF)	900–1700	PLSR	$R^2_{CV} = 0.83$	ElMasry, Barbin, et al. (2012)
		Colour (*L**)			$R^2_{CV} = 0.88$	
		Colour (*b**)			$R^2_{CV} = 0.81$	
		Marbling Level	400–1000	Decision Tree	$R^2_{P} = 0.99$	Velásquez et al. (2017)
		Marbling Level (Sensory)	400–1000	PLSR	$R^2_{P} = 0.95$	Aredo et al. (2017)
		Marbling Level (Sensory)	400–1100	MLR	$R^2_{CV} = 0.92$	Li et al. (2011)
		WHC	910–1700	PLSR	$R^2_{CV} = 0.89$	ElMasry et al. (2011)
		Colour (*L**)	400–1000	PLSR	$R^2_{P} = 0.887$	Liu et al. (2018)
		Colour (*a**)			$R^2_{P} = 0.864$	
Fish	Meat	Tenderness (WBSF)	400–1000	PLSR	$R^2_{P} = 0.901$	He et al. (2014a,b)
				LS-SVM	$R^2_{P} = 0.905$	
				MLR	$R^2_{P} = 0.901$	
			900–1700	PLSR	$R^2_{P} = 0.860$	
				LS-SVM	$R^2_{P} = 0.884$	
		Tenderness (WBSF)	400–1000	PLSR	$R^2_{P} = 0.9078$	Ma et al. (2017)
		Hardness (TPA)			$R^2_{P} = 0.9036$	
		Gumminess (TPA)			$R^2_{P} = 0.8774$	
		Chewiness (TPA)			$R^2_{P} = 0.8958$	
		Hardness (TPA)	400–1000	PLSR	$R^2_{CV} = 0.711$	Wu et al. (2014)
		Cohesiveness (TPA)			$R^2_{CV} = 0.567$	
		Adhesiveness (TPA)			$R^2_{CV} = 0.639$	
		Gumminess (TPA)			$R^2_{CV} = 0.711$	
		Chewiness (TPA)			$R^2_{CV} = 0.702$	
		Firmness (TPA)	400–1000	PLSR	$R^2_{P} = 0.899$	Cheng et al. (2014a)
				LS-SVM	$R^2_{P} = 0.932$	
		Hardness (TPA)	900–1700	PLSR	$R^2_{CV} = 0.67$	Wang et al. (2019b)
		Cohesiveness (TPA)			$R^2_{CV} = 0.72$	
		Springiness (TPA)			$R^2_{CV} = 0.72$	
		Gumminess (TPA)			$R^2_{CV} = 0.61$	
		Chewiness (TPA)			$R^2_{CV} = 0.62$	
		WHC	400–1000	PLSR	$R^2_{CV} = 0.834$	He et al. (2014a, 2014b)
			900–1700		$R^2_{CV} = 0.692$	
		Colour (*L**)	964–1631	MLR	$R^2_{P} = 0.869$	Wu et al. (2012)
		Colour (*a**)			$R^2_{P} = 0.729$	
		Colour (*b**)			$R^2_{P} = 0.788$	
		Freshness	400–1000	LS-SVM	$R^2_{P} = 0.944$	Cheng and Sun (2015)
		Freshness (TBA)	400–1000	MLR	$R^2_{P} = 0.839$	Cheng et al. (2015)
		Freshness (*K* Value)	400–1000	LS-SVM	$R^2_{P} = 0.922$	Cheng et al. (2015)
		Freshness (TVB-N)	400–1000	PLSR	$R^2_{P} = 0.905$	Cheng et al. (2014b)
		Freshness (TVB-N)	308–1105	PLSR	$R^2_{P} = 0.981$	Cheng et al. (2017)
		Freshness (TVB-N)	400–1000	PLSR	$R^2_{P} = 0.92$	Ivorra et al. (2016)
		Freshness (TVB-N)	900–1700	PLSR	$R^2_{CV} = 0.74$	Wang et al. (2019)
Lamb	Meat	Tenderness (WBSF)	900–1700	PLSR	$R^2_{CV} = 0.84$	Kamruzzaman et al. (2013)
				MLR	$R^2_{CV} = 0.84$	
		Tenderness (Sensory)		PLSR	$R^2_{CV} = 0.70$	
		WHC	900–1700	PLSR	$R^2_{CV} = 0.77$	Kamruzzaman et al. (2012)
		Colour (*L**)			$R^2_{CV} = 0.91$	
Pork	Meat	Tenderness (WBSF)	400–1100	MLR	$R^2_{CV} = 0.93$	Tao et al. (2012)
		Tenderness (SSF)	910–1700	PLSR	$R^2_{CV} = 0.75$	Barbin et al. (2013)
		Marbling Level	900–1700	MLR	$R^2_{CV} = 0.92$	Liu and Ngadi (2014)
				PLSR	$R^2_{CV} = 0.93$	
		WHC	900–1700	PLSR	$R^2_{P} = 0.89$	Barbin et al. (2012)
		Colour (*L**)			$R^2_{P} = 0.92$	
		Colour (*a**)			$R^2_{P} = 0.76$	
		Colour (*b**)			$R^2_{P} = 0.87$	
		Colour (Hue Angle)			$R^2_{P} = 0.80$	
		Colour (Chroma)			$R^2_{P} = 0.79$	
		WHC	400–1000	PLSR	$R^2_{P} = 0.591$	Xie et al. (2015)
			900–2500		$R^2_{P} = 0.740$	
		Colour (*L**)	400–1000	PLSR	$R^2_{P} = 0.907$	Xie et al. (2015)
		Colour (*a**)			$R^2_{P} = 0.716$	
		Colour (*b**)			$R^2_{P} = 0.814$	
		WHC	400–1100	MLR	$R^2_{C} = 0.92$	Wu and Yu (2015)
		Colour (*L**)			$R^2_{C} = 0.98$	
		Colour (*a**)			$R^2_{C} = 0.94$	
		Colour (*b**)			$R^2_{C} = 0.92$	
		Colour (*L**)	400–1000	PLSR	$R^2_{CV} = 0.751$	Liu et al. (2014)
		Colour (*a**)			$R^2_{CV} = 0.724$	
		Colour (*b**)			$R^2_{CV} = 0.528$	
		Freshness (TVB-N)	430–960	BP-AdaBoost	$R^2_{P} = 0.932$	Li et al. (2015)

(*continued on next page*)

Table 2 (*continued*)

Products	Food Type	Sensory features	Wavelengths (nm)	Models	Accuracy	References
		Freshness (K Value)	400–1100	PLSR	$R^2_P = 0.924$	Cheng et al. (2016)
		Freshness (BAI)	400–1000	MLR	$R^2_P = 0.957$	Cheng et al. (2016)
		Freshness (TVB-N)	400–1000	MLR	$R^2_P = 0.861$	Yang et al. (2017)
Pork Sausages	Meat	Colour (*L**)	380–1000	PLSR	$R^2_P = 0.73$	Feng and Makino (2020)
		Colour (*a**)			$R^2_P = 0.76$	
		Colour (*L**)	380–1000	PLSR	$R^2_{CV} = 0.76$	Feng et al. (2020)
		Colour (*a**)			$R^2_{CV} = 0.66$	
		Colour (*b**)			$R^2_{CV} = 0.71$	
		Colour (*a**)	380–1000	PLSR	$R^2_P = 0.792$	Feng et al. (2017)
				FSMR	$R^2_P = 0.758$	
Turkey Hams	Meat	Colour (*a**)	900–1700	PLSR	$R^2_{CV} = 0.74$	Iqbal et al. (2013)
Red Meat	Meat	WHC	400–1000	PLSR	$R^2_P = 0.92$	Kamruzzaman et al. (2016a,b)
				LS-SVM	$R^2_P = 0.94$	
		Colour (*L**)	400–1000	MLR	$R^2_P = 0.97$	Kamruzzaman et al. (2016a,b)
		Colour (*a**)			$R^2_P = 0.84$	
		Colour (*b**)			$R^2_P = 0.82$	
Chicken	Meat	Springiness (TPA)	400–1000	PLSR	$R^2_P = 0.89$	Xiong et al. (2015)
				ANN	$R^2_P = 0.84$	
		WHC	1000–2500	PLSR	$R^2_P = 0.80$	Yang et al. (2018)
		Colour (*L**)	400–1000	PLSR	$R^2_P = 0.75$	Jiang et al. (2018)
		Colour (*a**)			$R^2_P = 0.92$	
		Colour (*b**)			$R^2_P = 0.87$	
		Freshness (TBARS)	328–1115	PLSR	$R^2_P = 0.944$	Xiong et al. (2015b)
Prawn	Meat	Hardness (TPA)	400–1000	LS-SVM	$R^2_P = 0.824$	Dai et al. (2014)
		Gumminess (TPA)			$R^2_P = 0.874$	
		Chewiness (TPA)			$R^2_P = 0.835$	
		Freshness (TVB-N)	400–1000	BP-NN	$R^2_P = 0.966$	Dai et al. (2015)
Shrimp	Meat	Freshness	867–1700	ELM	$R^2_P = 0.98$	Ye et al. (2020)
Egg	Other Products	Freshness	380–1010	SVR	$R^2_P = 0.87$	Zhang et al. (2015)
		Freshness	900–1700	PLSR	$R^2_P = 0.85$	Suktanarak and Teerachaichayut (2017)
		Freshness	400–1000	SVM	$R^2_P = 0.78–0.98$	Yao et al. (2020)
Banana	Fruit	Firmness (TPA)	400–1000	MLR	$R^2_P = 0.9114$	Rajkumar et al. (2012)
		Firmness (TPA)	380–1023	PLSR	$R^2_P = 0.760$	Xie et al. (2018)
		Colour (*L**)			$R^2_P = 0.802$	
		Colour (*a**)			$R^2_P = 0.975$	
		Colour (*b**)			$R^2_P = 0.842$	
		Colour (*L**)	400–1000	PLSR	$R^2_P = 0.61$	Nguyen-Do-Trong et al. (2018)
		Colour (*a**)			$R^2_P = 0.53$	
		Colour (*b**)			$R^2_P = 0.83$	
		Maturity (Visually)	400–740	PLS-DA	$R^2_P = 0.933$	Pu et al. (2019)
Apple	Fruit	Firmness (MT)	400–1000	PLSR	$R^2_P = 0.828$	Wang et al. (2012)
		Firmness (MT)	500–1000	PLSR	$R^2_P = 0.950$	Mendoza et al. (2011)
		Firmness (MT)	400–1000	PLSR	$R^2_P = 0.862$	Zhu et al. (2013)
		Bruise	400–1000	RF	$R^2_P > 0.98$	Che et al. (2018)
		Bruise	400–1000	GS-SVM	$R^2_P = 0.925$	Tan et al. (2018)
		Bruise	900–1700	PLS-DA	$R^2_P = 0.56–0.96$	Ferrari et al. (2015)
		Bruise	400–1000	LDA	$R^2_P = 0.95$	Baranowski et al. (2012)
		Bruise	400–2500	LLR	$R^2_P = 0.926$	Baranowski et al. (2013)
		Bruise	900–2500	PLS-DA	$R^2_P = 0.86–0.94$	Keresztes et al. (2016)
		Flavour (Sweetness)	380–1040	SVR	$R^2_P = 0.887$	Liu et al. (2020)
		Flavour (Sourness)			$R^2_P = 0.81$	
Peach	Fruit	Chilling Injury (Sensory)	400–1000	ANN	$R^2_P = 0.85–0.99$	Sun et al. (2017b)
				SVM	$R^2_P = 0.71–0.96$	
				PLS-DA	$R^2_P = 0.65–0.96$	
				FLDA	$R^2_P = 0.53–0.93$	
		Chilling Injury (Sensory)	400–1000	ANN	$R^2_P = 0.958$	Pan et al. (2016)
		Bruise	780–2500	I-WSM	$R^2_{CV} = 0.965$	Li et al. (2018b)
Nectarine	Fruit	Maturity	450–1040	PLSR	$R^2_P = 0.87–0.91$	Munera et al. (2017)
Blueberry	Fruit	Firmness (TPA)	500–1000	PLSR	$R^2_P = 0.869$	Leiva-Valenzuela et al. (2013)
		Hardness (TPA)	410–1113	LS-SVM	$R^2_P = 0.8628$	Hu et al. (2015)
		Springiness (TPA)			$R^2_P = 0.7189$	
		Chewiness (TPA)			$R^2_P = 0.7929$	
		Resilience (TPA)			$R^2_P = 0.7851$	
		Bruise	950–1650	LS-SVM	$R^2_P = 0.75–1.0$	Fan et al. (2017)
		Bruise	950–1650	FCN	$R^2_P = 0.811$	Zhang et al. (2020)
		Maturity (Visually)	400–1010	KNN	$R^2_P = 0.987$	Yang et al. (2014)
Strawberry	Fruit	Maturity (Visually)	445–1020	SVM	$R^2_P = 0.933$	Zhang et al. (2016)
		Maturity (Visually)	370–1015	CNN	$R^2_P = 0.986$	Gao et al. (2020)
Cherry	Fruit	Firmness (TPA)	500–1600	PLSR	$R^2_P = 0.57$	Reddy and Li (2020)
				GPR	$R^2_P = 0.60$	
		Maturity	874–1734	LDA	$R^2_C = 0.964$	Li et al. (2018c)
Mango	Fruit	Firmness (TPA)	450–1000	PLSR	$R^2_{CV} = 0.81$	Rungpichayapichet et al. (2017)
Kiwifruit	Fruit	Hardness (TPA)	400–1000	PLSR	$R^2_P = 0.8738$	Chen et al. (2020)
		Firmness (TPA)	450–1000	MLR	$R^2_P = 0.9812$	Zhu et al. (2017)
				LS-SVM	$R^2_P = 0.9821$	
				PLSR	$R^2_P = 0.9746$	

(*continued on next page*)

Table 2 (*continued*)

Products	Food Type	Sensory features	Wavelengths (nm)	Models	Accuracy	References
			951–1670	PLSR	$R^2_P = 0.9579$	
		Bruise	408–1117	SVM	Not mentioned	Lü et al. (2011)
Plum	Fruit	Colour (*L**)	600–975	PLSR	$R^2_P = 0.85$	Li et al. (2018)
		Colour (*a**)			$R^2_P = 0.80$	
		Colour (*b**)			$R^2_P = 0.72$	
Pear	Fruit	Firmness (TPA)	400–1000	PLSR	$R^2_{CV} = 0.867$	Fan et al. (2015)
		Bruise	950–1650	*F*-value	$R^2_C = 0.92$	Lee et al. (2014)
		Maturity (Visually)	400–700	SVM	$R^2_P = 0.946$	Yu et al. (2020)
Pomegranate	Fruit	Maturity (Visually)	720–1050	PLS-DA	$R^2_P = 0.84–1.0$	Munera, Aleixos, et al. (2019)
Melon	Fruit	Flavour	900–1700	PLSR	$R^2_P = 0.57–0.80$	Sun et al. (2017)
Jujube	Fruit	Chilling Injury (Visually)	380–1023	LDA	$R^2_P = 0.93$	Lu et al. (2018)
		Bruise	850–1730	CCN	$R^2_P = 0.99–1.0$	Feng et al. (2019)
				LR	$R^2_P = 0.97–1.0$	
				SVM	$R^2_P = 0.98–1.0$	
Persimmon	Fruit	Flavour	450–1020	QDA	$R^2_P = 0.951$	Munera et al. (2017b)
		Maturity		SVM	$R^2_{CV} = 0.983$	
		Flavour	450–1040	PLS-DA	$R^2_P = 0.81–0.89$	Munera et al. (2019)
		Maturity	400–1000	LS-SVM	$R^2_P = 0.938$	Wei et al. (2014)
Orange	Fruit	Maturity	390–1055	KNN	$R^2_P = 0.96$	Wei et al. (2017)
Lime	Fruit	Maturity	930–1670	PLSR	$R^2_P = 0.78$	Teerachaichayut and Ho (2017)
Red Grape	Fruit	Flavour	950–1650	SLDA	$R^2_{CV} = 0.86$	Nogales-Bueno et al. (2015)
White Grape	Fruit	Flavour	884–1717	PLSR	$R^2_{CV} = 0.50–0.98$	Jara-Palacios et al. (2016)
Grape Seeds	Fruit	Flavour	950–1650	PLSR	$R^2_P = 0.75–0.88$	Rodríguez-Pulido et al. (2014)
Lychee	Fruit	Maturity	1000–2500	PLS-DA	$R^2_P = 0.968$	Pu et al. (2016)
Cucumber	Vegetable	Chilling Injury (Sensory)	500–1000	SVM	$R^2_C = 0.81–1.0$	Cen et al. (2016)
Tomato	Vegetable	Firmness (TPA)	1000–1550	PLSR	$R^2_P = 0.82$	Rahman et al. (2018c)
		Flavour (Sweetness)			$R^2_P = 0.74$	
		Colour (*L**)	400–1000	PLSR	$R^2_P = 0.86$	Roy et al. (2017)
		Colour (*a**)			$R^2_P = 0.93$	
		Colour (Hue Angle)			$R^2_P = 0.95$	
		Maturity (Visually)	500–950	PLS-DA	$R^2_{CV} = 0.80–0.88$	Zhu et al. (2015)
Potato	Vegetable	Colour (*L**)	380–1030	LS-SVM	$R^2_P = 0.858$	Xiao et al. (2020)
		Colour (*a**)			$R^2_P = 0.957$	
		Colour (*b**)			$R^2_P = 0.924$	
		Bruise	400–1000	SVM	$R^2_P = 0.73–0.94$	Ye et al. (2018)
		Bruise	400–1000	AdaBoost-FLDA	$R^2_P = 0.998$	Ji et al. (2019)
Mushroom	Vegetable	Bruise	880–1720	PLS-DA	$R^2_{CV} = 0.904$	Esquerre et al. (2012)
Green Bell Pepper	Vegetable	Chilling Injury (Sensory)	400–1000	PLS-DA	$R^2_{CV} = 0.83–0.96$	Babellahi et al. (2020)
			1000–2500		$R^2_{CV} = 0.63–0.84$	
Green Pepper	Vegetable	Flavour	1000–1600	PLSR	$R^2_P = 0.86$	Rahman et al. (2018)
Garlic	Vegetable	Flavour	1000–1700	PLSR	$R^2_P = 0.86$	Rahman et al. (2018)
				LS-SVM	$R^2_P = 0.87$	
Vegetable Soybean	Vegetable	Colour (ΔE)	400–1000	PLSR	$R^2_P = 0.862$	Huang et al. (2014)
Spinach Leaves	Vegetable	Freshness	380–1030	ELM	$R^2_P = 1.0$	Zhu et al. (2019)
Kernel Wheat	Other products	Hardness	1000–2500	PLSR	$R^2_P = 0.80$	Erkinbaev et al. (2019)
				ANN	$R^2_P = 0.90$	
		Hardness	900–1700	PLSR	$R^2_P = 0.8492$	Zhang et al. (2017)
				iPLSR	$R^2_P = 0.9174$	
				ACO	$R^2_P = 0.9544$	
Maize seed	Other products	Hardness (TPA)	400–1000	PLSR	$R^2_P = 0.9012$	Wang et al. (2015)
		Springiness (TPA)			$R^2_P = 0.8744$	
		Resilience (TPA)			$R^2_P = 0.8477$	
Canned black bean	Other products	Firmness (KSP)	400–1000	PLSR	$R^2_P = 0.844$	Mendoza et al. (2018)
Pistachio kernel	Other products	Hardness (TPA)	400–1000	PLSR	$R^2_P = 0.64$	Mohammadi-Moghaddam et al. (2018)
				ANN	$R^2_P = 0.88$	
Peanut	Other products	Maturity (Visually)	400–1000	FCLS	$R^2_P = 0.84–0.98$	Zou et al. (2019)
Tea Leaves	Other products	Colour (*L**)	380–1030	LS-SVM	$R^2_P = 0.931$	Xie et al. (2014)
		Colour (*a**)			$R^2_P = 0.973$	
		Colour (*b**)			$R^2_P = 0.933$	
		Flavour	450–1000	PLSR	$R^2_{CV} = 0.66$	Tu et al. (2018)
Cocoa Bean	Other products	Flavour	1000–2500	PLSR	$R^2_P = 0.70$	Caporaso et al. (2018)
Coffee Bean	Other products	Flavour (Caffeine)	980–2500	PLSR	$R^2_{CV} = 0.793$	Caporaso et al. (2018)
		Flavour (Trigonelline)			$R^2_{CV} = 0.733$	
Barley Malt	Other products	Flavour	1000–2500	SVR	$R^2_P = 0.98$	Tschannerl et al. (2019)
Hard Cheese	Other products	Maturity (Sensory)	1000–2400	PLSR	$R^2_P = 0.76$	Priyashantha et al. (2020)

Abbreviations: R^2_C = coefficients of determination in calibration; R^2_{CV} = coefficient of determination in cross-validation, R^2_P = coefficient of determination in prediction; MLR = multi-linear regression; PLSR = partial least squares regression; LS-SVM = least-squares support vector machine; BP-Adaboost = back propagation adaptive boosting algorithm; FSMR = forward stepwise multiple regression; ANN = artificial neural network; BP-NN = backpropagation neural network; ELM = extreme learning machine; SVR = support vector regression; SVM = support vector machine; PLS-DA = partial least square discriminant analysis; RF = random forest; GS-SVM = grid search-support vector machine; LDA = linear discriminant analysis; LLR = logistic linear regression; FLDA= Fisher linear discriminate analysis; I-WSM = improved watershed segmentation method; FCN = fully convolutional network; KNN=K-nearest neighbour; CNN = convolutional neural network; GPR = Gaussian process regression; LR = logistic regression; QDA = quadratic discriminant analysis; SLDA = stepwise linear discriminant analysis; iPLSR = interval partial least square regression; ACO = ant colony optimization; FCLS = fully constrained least squares; WBSF=Warner-Bratzler shear test; SSF = slice shear force test; WHC = water holding capacity; TPA = texture profile analysis; TBA = thiobarbituric acid; TVB-N = total volatile basic nitrogen; BAI = biogenic amine index; TBARS = thiobarbituric acid reactive; MT = Magness–Taylor penetration test; ΔE = color difference; KSP=Kramer shear press.

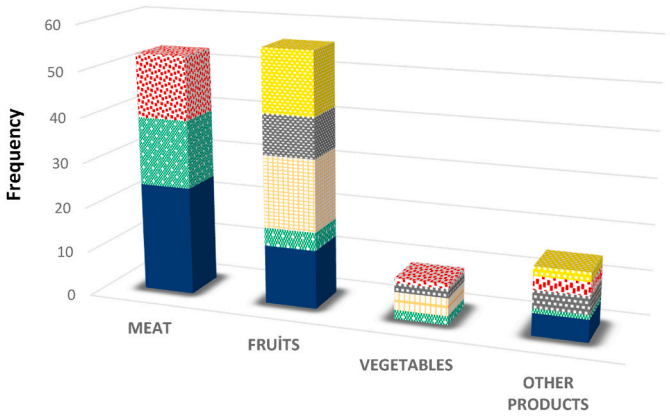

Fig. 3. The quantity of published studies for sensory assessment by hyperspectral imaging since 2010. (Texture, Colour, Defects, Flavour, Freshness, Maturity). (For interpretation of the references to colour in this figure legend, the reader is referred to the Web version of this article.)

different physical characteristics (Pathare et al., 2013). Therefore, researchers have sought out more automatic procedures to overcome these drawbacks.

Applications of estimation of colour features by HSI have been mostly focused on meat (Barbin et al., 2012; Jiang et al., 2018; Wu & Yu, 2015; Kamruzzaman et al., 2012; Liu et al., 2014; Lee et al., 2014; Wu, Sun, & He, 2012; Xie et al., 2015) and meat products (Feng & Makino, 2020; Feng et al., 2017, 2020; Iqbal et al., 2013), but many studies in fruits and vegetables (Huang et al., 2014; Li et al., 2018b; J. Li, Chen, & Huang, 2018a; X. Li et al., 2018c; Nguyen-Do-Trong et al., 2018; Roy et al., 2017; Xie et al., 2018), and tea (Xie et al., 2014) have also been demonstrated. Different wavelengths selection methods such as stepwise discrimination (Wu, Sun, & He, 2012), weighted β-coefficients (ElMasry, Sun, & Allen, 2012), successive projections algorithm (SPA) (Li, Cobo-Medina, et al., 2018), and competitive adaptive reweighted sampling (CARS) (Xiao et al., 2020) have been used for reducing redundant information and to simplify multivariate models. Xiao et al. (2020) performed a study to predict colour features of potatoes by PLSR and least-squares support vector machine (LS-SVM) with SPA and CARS. The CARS-LS-SVM model obtained the best performance with R^2_P of 0.851 for L^*, 0.957 for a^*, and 0.924 for b^*. In the study of Kamruzzaman, Makino, and Oshita (2016a,b), PLSR, LS-SVM, and MLR with SPA as a related-wavelengths selection method were implemented to compare their performances in the prediction of the colour of red meat. All models yielded good prediction results with R^2_P ranging from 0.94 to 0.97 for L^*, 0.84–0.95 for a^*, and 0.81–0.85 for b^*. Moreover, Liu et al. (2018) established a study to predict the colour of beef samples by PLSR, MLR, and LS-SVM with regression coefficients (RC), using different spectral pre-treatments including SG, MSC, SNV, and derivatives to compare their prediction performances and acquired R^2_P of 0.858 for prediction of L^* by SNV-PLSR, 0.890 for a^* by SG-RC-MLR, and 0.816 for b^* by MSC-LS-SVM. Furthermore, Xie et al. (2018) tested a novel model called two-wavelength combination for selection of optimal wavelengths to estimate colour features of bananas by PLSR and obtained good prediction results with R^2_P of 0.795 for L^*, 0.972 for a^*, and 0.773 for b^*.

Food processing technologies have been widely applied for improving food quality and extending shelf-life, however, they can lead to changes in the colour features. Many studies have been carried out to determine the colour features by HSI during different processing procedures such as freezing (Xie et al., 2015), cooking (Iqbal et al., 2013; Feng et al., 2020), pre-cooking (Feng et al., 2017), microwave heating (Li, Cobo-Medina, et al., 2018), drying (Huang et al., 2014; Nguyen--Do-Trong et al., 2018; Xie et al.,2014), and salting (Lee et al., 2014). In particular, Xie et al. (2014) performed a study to predict the colour changes of tea leaves during different drying periods (0, 4, 6, 8, and 10 min) and yielded a good classification performance with R^2_P ranging from 0.714 to 1.0 by LS-SVM.

Although almost all studies about the colour prediction by HSI has been investigated in reflectance mode, two studies (Wu, Sun, & He, 2012; Wu & Yu, 2015) on the scattering hyperspectral imaging for colour assessment have shown more accurate results because the scattering mode can be affected by the structural properties of a product, while the reflectance mode contains only the spectral data of the product without tracking the spatial information. Moreover, as a linear algorithm, PLSR has been the most used method in the colour assessment by HIS, but non-linear algorithms such as LS-SVM has provided more robust results. This might be due to the remarkable performance of LS-SVM, which can not only analyse the linear correlation between the colour of the product and the spectral information, but can also better discover the nonlinear relationship between them.

3.2. Defects

3.2.1. Chilling injury

Chilling injury is one of the most common physiological disorders in fruits and vegetables, which can occur during low-temperature long term storage, and can cause various alterations such as internal browning, deteriorated texture, lack of juiciness, and off-flavour (Lurie & Crisosto, 2005). Hence, it is important to detect chilling injury in fruits and vegetables before reaching the consumers. Although chilling injury cannot be assessed directly by instruments, many properties are used as indices to predict the degree of chilling injury, including flesh colour, firmness, and dry matter (Cen et al., 2016).

In recent years, HSI in the spectral range of 400–1000 nm has been studied for the detection of chilling injury in early stages to remove injured agri-food products such as peaches (Pan et al., 2016; Sun, Zhang, et al., 2017), cucumbers (Cen et al., 2016), green bell peppers (Babellahi et al., 2020), and green jujubes (Lu et al., 2018), in order to improve the shelf-life of food products and to ensure the contentment of consumers. For example, Sun et al. (2017b) performed a study to classify the chilling injury of peaches by PLS-DA, SVM and ANN with SPA as optimal wavelengths selection method, and achieved the best performances with R^2_P of 0.866, 0.934, 0.967 by ANN for four-class, three-class and two-class classification, respectively. This result showed that the relationship between the chilling injury and the spectral information was too sophisticated to be solved by a linear multivariate algorithm, thus non-linear multivariate analysis should accomplish better performances. Furthermore, Cen et al. (2016) examined mutual information feature selection (MIFS), max-relevance min-redundancy (MRMR), and sequential forward selection (SFS) for selecting related-wavelengths, and the naïve Bayes (NB), SVM and K-nearest neighbour (KNN) for determining chilling injury of cucumbers for two-class and three-class classifications, creating models based on both spectral analysis and image analysis such as the first-order statistics and the second-order statistics. The images of the sample products and the main steps of this study are illustrated in Fig. 4. The study showed that SFS-SVM obtained the most accurate results among all classification models with an accuracy of $R^2_C > 0.90$ based on spectral features. The performances of classification models using features fusion based on image features extracted from the selected two-band ratio images were found to be comparable to the models based on spectral information. For further studies, the combination of spectral and image features could provide more accurate performances for classification of chilling injury.

3.2.2. Bruises

Bruising is mechanical damage in fruits and vegetables, which can occur during harvesting, packing, and transporting, affecting not only

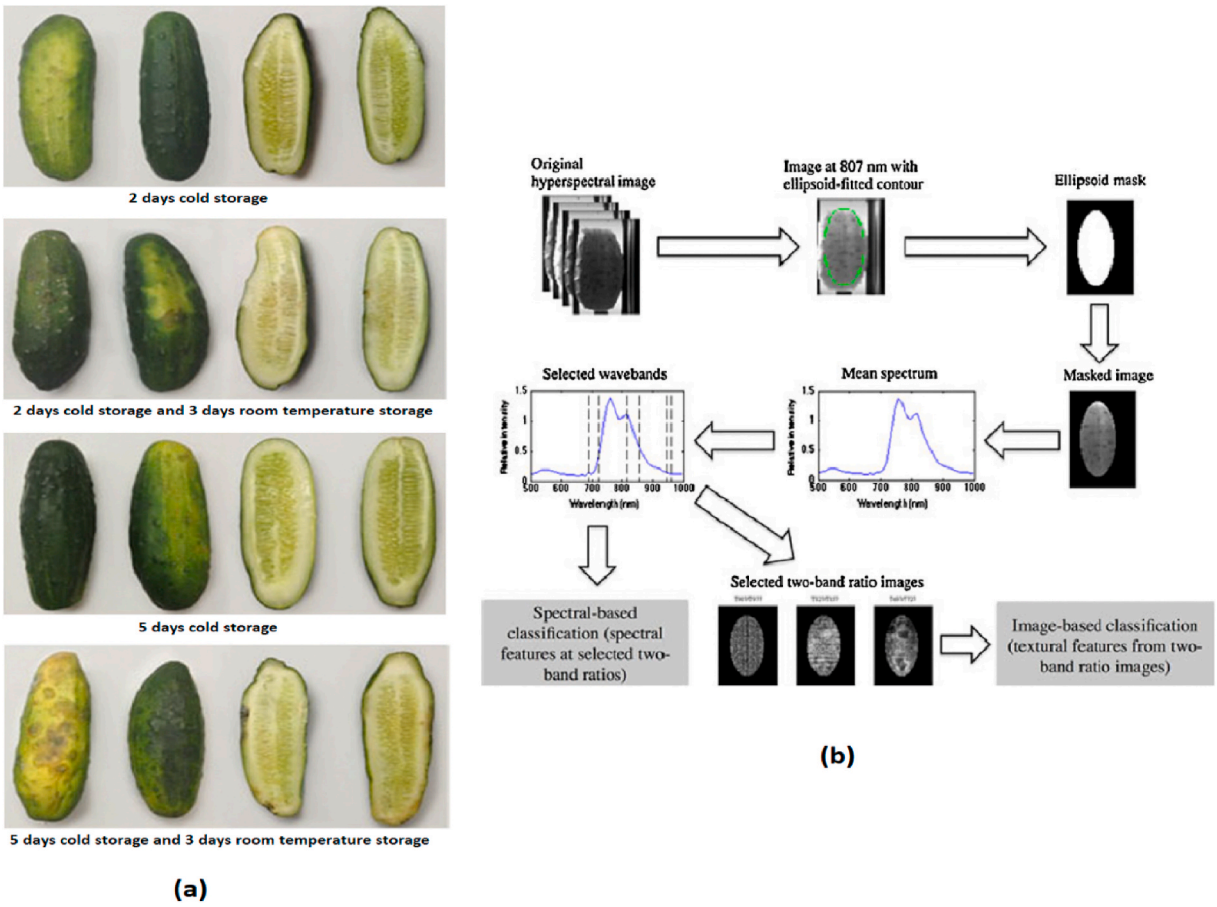

Fig. 4. Evaluation of chilling injury of cucumbers by HSI (a) sample image (b) key steps of image analysis process (Cheng, Sun, Pu, & Liu, 2016).

the appearance of foods but also its taste, texture, nutritional value, and consumer acceptance. Traditionally, bruises are classified by manual grading in the food industry, consequently, researchers have focused on finding self-regulating sorting systems for the early detection of bruises to decrease economic and nutritional value losses, and HSI has been investigated to detect bruises in apples (Ferrari et al., 2015; Keresztes et al., 2016), potatoes (Ji et al., 2019; Ye et al., 2018), pears (Lee et al., 2014), blueberries (Fan et al., 2017; Zhang & Li, 2018), peaches (Li, Cobo-Medina, et al., 2018), kiwifruits (Lü et al., 2011), winter jujubes (Feng et al., 2019), and mushrooms (Esquerre et al., 2012).

Che et al. (2018) detected bruises of apples with a pixel-based selection of the region of interest (ROI) and applied SVM, decision tree, stochastic gradient descent, random forests, and gradient tree boosting to create classification models, acquiring the best accuracy with R^2_P of 0.99 by random forests. In addition, Tan et al. (2018) applied SVM based on grid search parameter optimization (GS-SVM) with three spectral pre-processing methods including SNV, first derivative and SG smoothing, and their combinations to identify the bruises of apples after the selection of the effective wavelengths by SPA or CARS. They achieved the highest classification accuracy using SNV-SPA-GS-SVM with R^2_P of 0.95. On the contrary, Fan et al. (2017) performed a study using SPA and CARS with LS-SVM for the classification of bruises of blueberries and CARS-LS-SVM showed better performance. In the applications, the SPA has more wavelengths than CARS and thus better performance can be expected. However, in some studies, poorer classification ability has been shown, which could be because of the existence of some surplus or irrelevant information selected by SPA.

Other classification methods such as SIMCA (Baranowski et al., 2012), logistic linear regression (LLR) and neural network (NN) (Baranowski et al., 2013) have also been developed, which can yield good classification results. Recently, Ji et al. (2019) detected the early bruises of potatoes by HSI with image enhancement applications, including histogram equalization algorithm, mean smoothing and gradient algorithm. After applying discrete wavelet transform (DWT), the adaBoost-Fisher linear discriminant algorithm (FLD), KNN, FLD, backpropagation algorithm (BP) and SVM were applied for classification, and the best classification accuracy was achieved with R^2_P of 0.998 by histogram equalization with the adaBoost-FLD.

4. Evaluation of tactile sensory features of food products

4.1. Textural features

Food texture represents the ability of resistance of foods to deformation actions such as biting, chewing, and grinding (Lu & Cen, 2013), which can directly affect the acceptability of food and consumer preferences. The texture expectations of consumers widely diversify based on food products. For instance, consumers generally prefer apples to be firm, peaches to be juicy, and meat products to be tender (Chen & Rosenthal, 2015). Consequently, hardness, tenderness, juiciness, chewiness, and gumminess are the terms used for describing different food products (Szczesniak, 2002). Traditionally, besides trained panellists, many instrumental procedures are applied for textural assessments such as Warner–Bratzler shear test (WBSF), slice shear force (SSF) test, Magness–Taylor (MT) penetration test and texture profile analysis (TPA). In general, WBSF and SSF are used for evaluating the tenderness of meat while MT is applied for the firmness of fruits and vegetables. In addition, TPA is utilized for different food products to obtain primary textural parameters such as hardness, springiness, cohesiveness, adhesiveness and secondary parameters, including chewiness and gumminess

(De Huidobro et al., 2005). In recent years, HSI has been studied for replacing the traditional methods to evaluate these textural parameters.

The tenderness of meat simply is a textural characteristic related to the required biting force, changing based on the length of the sarcomere, degree of proteolysis (myofibrillar proteins), and the structure, or content of the connective tissue (Purchas, 2014). Consumers expect meat to have good quality tenderness as they can discriminate the level of tenderness efficiently (Feuz et al., 2004). HSI has been widely investigated to predict the tenderness (WBSF and SSF) of beef (ElMasry, Sun, & Allen, 2012; Wu, Sun, & He, 2012), pork (Barbin et al., 2013; Tao et al., 2012; Xie et al., 2015), fish (He, Wu, & Sun, 2014a, 2014b; Ma et al., 2017) and lamb (Kamruzzaman et al., 2013).

Studies on using HSI in meat tenderness evaluation are normally in the spectral range of 400–1100 nm and show good performances, such as R^2_{CV} of 0.91 by MLR (Wu, Sun, & He, 2012), 0.89 by PLSR and 0.905 by LS-SVM (He et al., 2014a,b). Tao et al. (2012) performed a hyperspectral scattering imaging for the prediction of tenderness (WBSF) of pork and acquired R^2_P ranging from 0.831 to 0.930 based on Lorentzian parameters. These good results could provide evidence to support the claim in previous studies that scattering imaging within meat was affected by muscle structural characteristics including the length of sarcomere and collagen content that are related to tenderness. Barbin et al. (2013) combined HSI and computer vision imagery for the estimation of tenderness (SSF) of pork and obtained reasonable prediction result with R^2_P of 0.75 from a PLSR model based on spectral information and statistical features from discrete wavelet transforms, which was higher than a PLSR model based on spectral data alone.

Furthermore, HSI has also been examined to predict TPA scores, including the hardness, gumminess, and chewiness of meat products (Dai et al., 2014; Wang, Russel, et al., 2019; Wu et al., 2014; Xiong, Sun, Pu, et al., 2015), the firmness of bananas (Rajkumar et al., 2012; Xie et al., 2018), apples (Mendoza et al., 2011; Zhu et al., 2013), blueberries (Leiva-Valenzuela et al. 2013), sweet cherries (Reddy & Li, 2020), melons (Sun, Zhang, et al., 2017), mangos (Rungpichayapichet et al., 2017), kiwifruits (Chen et al., 2020), pears (Fan et al., 2015), tomatoes (Rahman, Faqeerzada, & Cho, 2018), and the hardness of wheat kernels (Erkinbaev et al., 2019), maize seeds (Wang et al., 2015), pistachio kernels (Mohammadi-Moghaddam et al., 2018), and canned black beans (Mendoza et al., 2018). Many methods have been applied for selecting texture-related wavelengths such as RC (Ma et al., 2017), uninformative variable elimination (UVE) and supervised affinity propagation (SAP) (Wang et al., 2012), random frog algorithm (RFA) (Hu et al., 2015), variable importance in projection (VIP) (Rahman, Faqeerzada, & Cho, 2018) and genetic algorithm (GA) (Cheng, Qu, Sun, & Zeng, 2014a; Cheng, Sun, Zeng, & Pu, 2014b).

Wang et al. (2015) predicted the textural properties of maize kernel seeds by PLSR in the spectral range of 400–1000 nm. Before PLSR modelling based on full wavelengths, spectral correction using orthogonal signal correction (OSC) was used, which yielded good prediction results with R^2_P of 0.9012, 0.8744, 0.8477 for the estimation of hardness, springiness and resilience, respectively. Another study about the prediction of the firmness of kiwifruits was utilized by Zhu et al. (2017), who compared the performances of PLSR, MLR and LS-SVM models, and achieved the highest R^2_P of 0.9821 by SPA-LS-SVM. Moreover, ant colony optimization (ACO) and interval partial least squares regression (iPLSR) (Zhang et al., 2017), synergy interval PLSR (siPLSR) (Chen et al., 2020), backpropagation neural network (BP-NN) (Wang et al., 2012) have also been used for predicting textural features and show good prediction results with R^2_P of 0.828–0.9544.

Besides the evaluation of the textural properties of raw food products, the determination of the textural characteristics of processed foods is similarly essential to identify any sensory loss during processing. Therefore, HSI has been implemented to determine textural changes during different processes such as freezing (Xie et al., 2015), vacuum freeze-drying (Ma et al., 2017), frozen storage (Cheng, Qu, Sun, & Zeng, 2014a; Cheng, Sun, Zeng, & Pu, 2014b), canning (Mendoza et al., 2017), cooking (Kamruzzaman et al., 2013), and roasting (Mohammadi-Moghaddam et al., 2018), and results from these studies demonstrated encouraging performances in using HSI to predict textural features of processed food products.

4.2. Texture-related features

4.2.1. Marbling level

Marbling is a meat quality characteristic to determine the size, number, and distribution of visible fat with lean in a muscle, which is closely related to textural properties such as tenderness and juiciness (Corbin et al., 2015; Miller, 2014; Thompson, 2004). The uniform distribution of marbling is considered as an indicator of good quality meat by consumers. Traditionally, marbling is assessed visually by trained graders in accordance with marbling reference standards. On the other hand, HSI has been explored to be an alternative technique to determine the marbling level of meats such as beef (Aredo et al., 2017; Li et al., 2011; Velásquez et al., 2017) and pork (Cheng, Sun, Pu, & Wei, 2018; Liu & Ngadi, 2014; Ma, Pu, & Sun, 2018), showing good prediction results with coefficients of determination ranging from 0.92 to 0.99. Recently, a model of the decision tree was applied to eliminate some limitations of multivariate methods about generating binary images and more accurate results with $R^2_P = 0.99$ were achieved with the binarization of the region of interest (Velásquez et al., 2017). In addition, PLSR and MLR models were employed to estimate marbling scores with R^2_p of 0.95, and 0.92, respectively (Aredo et al., 2017; Li et al., 2011).

4.2.2. Water holding capacity

Water holding capacity (WHC) or drip-loss (DL) of meat is identified as the capability of the meat to maintain the water inside against external factors such as gravity and temperature (Fischer, 2007). Although it seems like a chemical property, WHC is a characteristic, providing information about the juiciness and tenderness of fresh or cooked meat and consequently, the total eating quality. Many methods have been used for evaluation of WHC, including external mechanical force, gravimetric and cooking procedures (Bowker, 2017). However, a fast and less repeatable procedure is an urgent need for the meat industry, and thus, the availability of HSI for the estimation of WHC in the spectral range of 400–1000 nm (Cheng, Sun, & Pu, 2016c; He et al., 2014a, 2014b; Kamruzzaman et al. (2016a,b); Ma, Sun, & Pu, 2017; Wu & Yu, 2015; Xie et al., 2015), and 900–2000 nm (Barbin et al., 2012; ElMasry et al., 2011; Kamruzzaman et al., 2012; Yang et al., 2018) has been investigated by many researchers. In particular, Barbin et al. (2012) established a PLSR model to compare effects of spectral pre-treatments on the prediction ability and reported that the best prediction R^2_P of 0.89 was obtained by the application of 1st derivate. This prediction coefficient was significantly higher than R^2_P of 0.77 that was obtained by PLSR based on raw spectral data (Kamruzzaman et al., 2012). This result has shown that image pre-processing could improve the prediction ability of multivariate analysis but it is a disadvantage in applications that the selection of the pre-treatment method is only based on trial and error. Besides PLSR, LS-SVM (Kamruzzaman et al., 2016a,b) and MLR (Wu & Yu, 2015) were also used for the prediction of WHC and yielded acceptable prediction coefficients ranging from 0.78 to 0.94. Recently, Yang et al. (2018) estimated the WHC of chicken breast fillets by PLSR and acquired R^2_p of 0.73, and for improving the prediction, fused the data of optimal wavelengths and texture variables extracted by grey level co-occurrence matrix (GLCM) and achieved more robust results with $R^2_P = 0.80$.

5. Evaluation of multisensory features of food products

5.1. Flavour

Flavour is a sensory impression of food products, which is identified by the combined chemical senses of the taste and smell system, and

flavour perception can thus be summarized in three stages: odour evaluation, the flavour in the mouth and aftertaste. Fundamentally, there are five taste classes, including sweetness, saltiness, sourness, bitterness, and umami perceived by the mouth, however, a wide range of flavours are formed with the combination of taste and odorants (Choi & Han, 2015, pp. 1–14). The assessments of flavour are generally implemented by trained panellists or instrumental methods such as gas chromatography-mass spectrometry, but it is hard to detect due to the trace amount of odorants. Therefore, HSI has been introduced for obviating this challenge by combining spectral and spatial information. Many flavour-related studies have been investigated by HSI for the prediction of astringency of persimmon (Munera et al., 2017; Munera et al., 2017), the phenolic content (related to the bitterness and sourness) in red and white grape seeds (Rodríguez-Pulido et al., 2014), single cocoa beans (Caporaso, Whitworth, Fowler, & Fisk, 2018), malted barley (Tschannerl et al., 2019), skins, seeds and stems of white grapes (Jara-Palacios et al., 2016), and tea cultivars (Tan et al., 2018), the anthocyanin content (related to the bitterness) of red grapes (Nogales-Bueno et al., 2015), the sweetness of melons (Sun, Zhang, et al., 2017) and tomatoes (Rahman, Faqeerzada, & Cho, 2018), the sweetness and sourness of apples (Liu et al., 2020), the pungency of green pepper (Rahman, Faqeerzada, & Cho, 2018), the allicin content of garlic creating the special flavour of garlic (Rahman, Faqeerzada, & Cho, 2018), and the flavour-related components of single green coffee beans (Caporaso, Whitworth, Fowler, & Fisk, 2018).

Jara-Palacios et al. (2016) performed a study to predict 27 individual phenolic compounds of seeds, skins, and stems of white grapes by HSI in the spectral range of 880–1720 nm with PCA-PLSR, and acquired good prediction results, especially for epicatechin (R^2_{cv} = 0.96), kaempferol-3-O-galactoside (R^2_{cv} = 0.98), kaempferol-3-O-glucoside (R^2_{cv} = 0.98), and kaempferol (R^2_{cv} = 0.97). Moreover, Rahman, Faqeerzada, and Cho (2018) demonstrated the prediction of the allicin content in garlic in the Vis-NIR (400–1000 nm) and NIR (1000–1700 nm) region. They employed different chemometrics to compare their effects on prediction, including five different spectral pre-treatments (normalization, MSC, SNV, SG-1st, SG-2nd), three-wavelength selection methods (RC, VIP, SPA), and two multivariate analysis (PLSR, LS-SVM). Their results showed that the NIR region with SG-1st application obtained more accurate prediction results and the best prediction results were R^2_P = 0.87 from an LS-SVM model based on full wavelengths, and R^2_p = 0.83 from a VIP-LS-SVM model. This might be because both NIR spectra are more related to the chemical composition of the samples and Vis-NIR spectra can be affected by some factors including colour and shape. Recently, Liu et al. (2020) applied particle swarm optimization-support vector regression (PSO-SVR) with CARS for wavelength selection to predict the sourness and the sweetness of apples and obtained R^2_P of 0.810, and 0.887 for the prediction of the sourness, and the sweetness, respectively.

5.2. Freshness

Freshness is a multisensory (olfactory, gustatory, tactile, trigeminal, visual, and auditory) characteristic, which can affect the acceptability and total quality of food products. It is a very broad concept since the expectations of consumers differentiate according to the type of foods (Roque et al., 2018). For instance, people consider that fresh fruits should have bright colour and expected texture, while fresh red meats should have red colour and good smell. Accordingly, studies have shown that there is a correlation between freshness and sensory properties, such as the appearance, texture, taste and smell (Howgate, 2015; Péneau et al., 2006). There are many procedures to be used for evaluating the freshness, including physical methods such as texture and colour analyses, chemical methods such as biogenic amine index and total volatile basic nitrogen, and microbiological analysis, however, for more precise determination, sensory panels are the only method (Wang et al., 2018). In order to overcome the difficulty, HSI has been examined for the potentiality and feasibility in accurate freshness evaluation and thus many studies have been conducted, mainly for meat and meat products (Cheng, Sun, Pu, & Zhu, 2015; Cheng et al., 2017; Cheng, Qu, et al., 2014; Cheng, Sun, Pu, & Zhu, 2015; Cheng, Sun, Pu, & Liu, 2016; Ivorra et al., 2016; Dai, Cheng, Sun, Zhu, & Pu, 2016; Li et al., 2015; Xiong, Sun, Pu, et al., 2015; Yang et al., 2017), eggs (Suktanarak & Teerachaichayut, 2017; Zhang et al., 2015), and spinach leaves (Zhu et al., 2019).

Cheng, Sun, and Cheng (2016) predicted pork freshness by HSI with different pre-treatments (MSC, SNV, and SG smoothing), wavelength selection algorithms (SPA and RC) and two multivariate analyses (PLSR and MLR), and their performances were compared, revealing that the SG smoothing-MLR achieved the best prediction performance with R^2_P of 0.957 based on nine optimal wavelengths selected by RC. In the studies to estimate the freshness, LS-SVM (Cheng & Sun, 2015), PLS-DA, random forest (RF), extreme learning machine (ELM) (Ye et al., 2020), clustering-based partial least squares (C-PLSR) (Wang, Russel, et al., 2019), and AdaBoost and BP-NN (Dai et al., 2015) have also been applied with good prediction R^2_P ranging from 0.74 to 0.981. Most recently, Yao et al. (2020) detected the freshness of eggs by HSI in the spectral range of 400–1000 nm. They used different image pre-processing methods such as Mahalanobis distance (MD), SG, SNV, and wavelet threshold denoising (WTD), and three different wavelength selection algorithms including iteratively retains informative variables (IRIV), CARS, and variable iterative space shrinkage approach (VISSA). After WTD-SNV application, which was found to be the best method for denoising and smoothing the spectra (Fig. 5), IRIV-SVM optimized by GA showed the best accuracy in test samples with R^2_P of 0.9787, which was significantly higher than IRIV-SVM (R^2_P = 0.8936).

5.3. Maturity

Maturity or ripeness is a stage that can show the readiness of foods for eating, which can be defined by both the internal and external characteristics of the food products. Moreover, food products can gain the desirable sensory characteristics such as palatable taste, intended texture, and specific colour during ripening (Cascales et al., 2005; Cliff & Toivonen, 2017). For instance, some products such as persimmon and banana are unlikely to be consumed before they reach maturity because of their astringency taste and hard texture. Therefore, the determination of the maturity stage of foods can guarantee the sensory quality, leading to the maintenance of market share by ensuring consumer satisfaction. Generally, the ripeness assessment can be determined by trained panels or laboratory-based parameters such as colour, texture, and total solid content. However, it is obvious that online monitoring systems are needed in the industry, and thus HSI has been widely investigated for the classification and prediction of the maturity stages of foods such as cheese (Priyashantha et al., 2020), peanut (Zou et al., 2019), persimmon (Wei et al., 2014), cherry (Li, Cobo-Medina, et al., 2018), strawberry (Gao et al., 2020), tomato (Zhu et al., 2015), lime (Teerachaichayut & Ho, 2017), pomegranate (Munera, Aleixos, et al. (2019)), orange (Wei et al., 2017), lychee fruit (Pu et al., 2016), and pear (Yu et al., 2020).

Yang et al. (2014) classified the maturity of blueberry in the spectral range of 400–1000 nm and used pair-wise class discriminability (PWCD), hierarchical dimensionality reduction (HDR), and non-Gaussianity measures (NG) algorithms for band selection, and KNN, SVM, and adaBoost as classification methods. All models yielded good classification accuracy with $R^2_P > 0.88$, but the best result was obtained with R^2_P = 0.987 by NG-KNN. Furthermore, Zhang et al. (2016) used two different spectral ranges of 380–1030 nm and 874–1734 nm and compared the classification performances among different models based on full spectra, optimal wavelengths selected by PCA, textural features extracted by GLCM and data fusion, respectively. They showed that the spectral range of 380–1030 nm yielded more accuracy than the other range and the best classification performance was R^2_P of 0.95 from an SVM model based on data fusion. The reason might be that the effect of

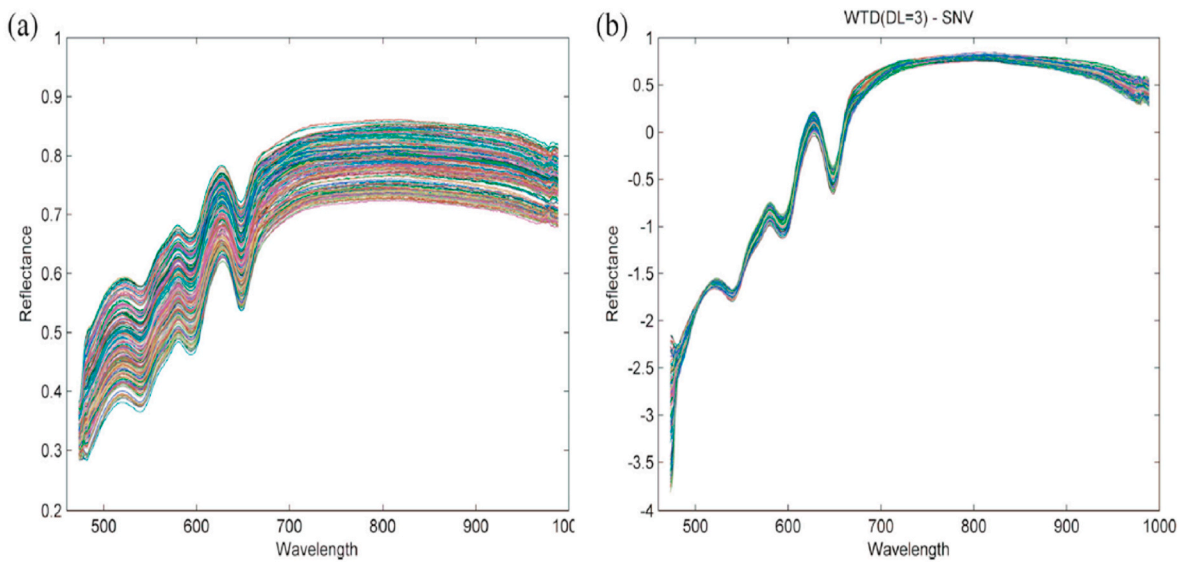

Fig. 5. Spectral curves for prediction of the freshness of eggs by HSI (a) original spectra (b) spectra after WTD-SNV application (Yao et al., 2020).

pigments, which was observed in the Vis-NIR range among different ripening stages, was more significant than chemical compositions. Besides these multivariate analysis, LDA, quadratic discriminant analysis (QDA) (Munera et al., 2017), PLSR (Munera et al., 2017), PLS-DA, SIMCA (Pu et al., 2019) have also been applied for classifying maturity levels with good accuracies ranging from 0.71 to 1.0.

6. Challenges and future work

In this review, the recent application developments of hyperspectral imaging technology since 2010 are enlightened in the assessment of sensory properties of various food products, confirming that hyperspectral imaging technology would have great potentials as a fast and noninvasive tool for sensory analysis.

Although hyperspectral imaging technology has shown great performances to predict the sensory evaluation of agri-food products, there are still some challenges that should be considered in future studies:

(1) The reflectance mode is most commonly used for image acquisition in sensory evaluation studies, however, it is a challenge to use this mode to achieve accurate analysis for food products with a round shape such as fruits. Recently, the scattering mode is also applied and showed more accuracy than the reflectance mode, but applications of other image acquisition modes are very limited in sensory assessment and thus the investigation of these modes is needed in future studies.

(2) Approximately 70% of the applications of HSI in the sensory assessment are carried out in the spectral range of 400–1000 nm, while only about 25% are in the spectral range of 900–1700 nm. However, the applications of HSI in the spectral regions such as UV (220–400 nm), SWIR (1000–2500 nm), and MWIR (3500–5000 nm) are very limited, hence the performances of these spectral ranges remain an enigma. For this reason, future studies can explore the feasibility of these spectral ranges in order to further advance this technology.

(3) Since most studies focus on analyzing spectral data and some studies have already indicated the success of the combination of spectral and spatial information, therefore more studies should be conducted on using data fusion techniques. GLCM is the most used method to extract the spatial information in the sensory analysis, but the feasibility of other methods such as Gabor filter, two-dimensional discrete wavelet transform and local binary pattern should also be investigated to improve the robustness of the technology.

(4) As hyperspectral images contain a large number of data with redundant information and high cost, effective data digging for extracting the most useful information remains a challenge for reducing computation cost and enhancing system performance. The selection of effective wavelengths is the most used method in overcoming this challenge. However, other methods should be studied and developed, for example, implementing the re-selection of optimal wavelengths to seek the most important wavelengths can help the building of multispectral imaging systems so that multi-band spectral cameras can be employed, which is more practical for industrial applications with regards to speed and cost. The use of multi-band spectral cameras could also be integrated with smartphones, leading to the adoption of this technology for daily life applications.

(5) To be undisputed in the efficiency of HSI technology for sensory evaluation, food products which have not been studied yet such as viscous products should be explored and studies should also be extended to a broader range of food products from different origins and geographical areas, considering that food products in the same category can have very different characteristics such as shapes and sizes.

(6) Currently, HSI systems are expensive, and it is a challenge to reduce their costs. Therefore, new technological developments in hardware such as sensors and illumination units are required. Besides, the software also has high selling prices and finding new software or approaches that are capable of performing similar functions as MATLAB or ENVI can further facilitate the reduction of the cost of this technology.

(7) Most studies on the application of hyperspectral imaging in the sensory evaluation are limited in the laboratory. Before the application of industrial-scale HSI, prototypes can be used in the sensory assessment with few modifications in the equipment such as using a micro stage to adjust the sample distances based on different sizes and shapes of samples, using a thermoelectric cooling system to reduce system noises based on the increasing operation temperature, and using a long conveyor belt to simulate real-time online image acquisition.

(8) Finally, the success of HSI in food sensory analysis is mainly in the laboratory, and the early translation of the laboratory results to industrial applications is challenging. However, with the rapid developments in the technology especially in both hardware and

software, it is expected that HSI technology should become an alternative tool for effective and efficient evaluation of sensory properties of food products for the food industry in future.

7. Conclusions

This review provides a comprehensive overview of recent application developments since 2010 for identifying sensory properties including texture, colour, defects, flavour, freshness, and maturity in various food products by hyperspectral imaging technology. For sensory evaluation, the most used spectral region is Vis-NIR (400–1000 nm), while the most applied multivariate analysis is linear regression models (PLSR and MLR). However, some non-linear regression algorithms can yield more accurate results. The supervised classification methods are mainly applied for detecting the defects and maturity of food products with the most accurate results in sensory evaluation by HSI. On the other hand, the regression multivariate analysis is widely used to predict texture, colour, flavour, and freshness. Besides many studies focus on reducing data redundancy and improving prediction performances by employing novel chemometric analyses, developing new algorithms, or selecting optimal wavelengths using different algorithms, however, the selection of effective wavelengths causes a major issue of losing information in some studies. Furthermore, combining spectral and spatial information of hypercubes for the evaluation of sensory properties can lead to better performances. In addition, some studies have proved the success of real-time hyperspectral imaging, which can encourage the early adoption of HSI technology by the industry.

Acknowledgements

Gözde Özdoğan is grateful to the YLSY Scholarship Programme, Ministry of National Education, Turkey, for a scholarship to support her PhD study in University College Dublin, Ireland.

References

Aredo, V., Velásquez, L., & Siche, R. (2017). Prediction of beef marbling using hyperspectral imaging (HSI) and partial least squares regression (PLSR). *Scientia Agropecuaria, 8*(2), 169–174. https://doi.org/10.17268/sci.agropecu.2017.02.09

Babellahi, F., Paliwal, J., Erkinbaev, C., Amodio, M. L., Chaudhry, M. M. A., & Colelli, G. (2020). Early detection of chilling injury in green bell peppers by hyperspectral imaging and chemometrics. *Postharvest Biology and Technology, 162*, 111100. https://doi.org/10.1016/j.postharvbio.2019.111100

Baranowski, P., Mazurek, W., & Pastuszka-Woźniak, J. (2013). Supervised classification of bruised apples with respect to the time after bruising on the basis of hyperspectral imaging data. *Postharvest Biology and Technology, 86*, 249–258. https://doi.org/10.1016/j.postharvbio.2013.07.005

Baranowski, P., Mazurek, W., Wozniak, J., & Majewska, U. (2012). Detection of early bruises in apples using hyperspectral data and thermal imaging. *Journal of Food Engineering, 110*(3), 345–355. https://doi.org/10.1016/j.jfoodeng.2011.12.038

Barbin, D. F., ElMasry, G., Sun, D. W., & Allen, P. (2012). Predicting quality and sensory attributes of pork using near-infrared hyperspectral imaging. *Analytica Chimica Acta, 719*, 30–42. https://doi.org/10.1016/j.aca.2012.01.004

Barbin, D. F., Valous, N. A., & Sun, D.-W. (2013). Tenderness prediction in porcine longissimus dorsi muscles using instrumental measurements along with NIR hyperspectral and computer vision imagery. *Innovative Food Science & Emerging Technologies, 20*, 335–342. https://doi.org/10.1016/j.ifset.2013.07.005

Bowker, B. (2017). Developments in our understanding of water-holding capacity. In M. Petracci, & C. Berri (Eds.), *Poultry quality evaluation: Quality attributes and consumer values* (pp. 77–113). Duxford, United Kingdom: Woodhead Publishing. https://doi.org/10.1016/B978-0-08-100763-1.00004-0.

Caporaso, N., Whitworth, M. B., Fowler, M. S., & Fisk, I. D. (2018a). Hyperspectral imaging for non-destructive prediction of fermentation index, polyphenol content and antioxidant activity in single cocoa beans. *Food Chemistry, 258*, 343–351. https://doi.org/10.1016/j.foodchem.2018.03.039

Caporaso, N., Whitworth, M. B., Grebby, S., & Fisk, I. D. (2018b). Non-destructive analysis of sucrose, caffeine and trigonelline on single green coffee beans by hyperspectral imaging. *Food Research International, 106*, 193–203. https://doi.org/10.1016/j.foodres.2017.12.031

Cascales, A. I., Costell, E., & Romojaro, F. (2005). Effects of the degree of maturity on the chemical composition, physical characteristics and sensory attributes of peach (*Prunus persica*) cv. Caterin. *Food Science and Technology International, 11*(5), 345–352. https://doi.org/10.1177/1082013205057943

Cen, H., Lu, R., Zhu, Q., & Mendoza, F. (2016). Nondestructive detection of chilling injury in cucumber fruit using hyperspectral imaging with feature selection and supervised classification. *Postharvest Biology and Technology, 111*, 352–361. https://doi.org/10.1016/j.postharvbio.2015.09.027

Cheng, J.-H., Qu, J.-H., Sun, D.-W., & Zeng, X.-A. (2014a). Visible/near-infrared hyperspectral imaging prediction of textural firmness of grass carp (*Ctenopharyngodon idella*) as affected by frozen storage. *Food Research International, 56*, 190–198. https://doi.org/10.1016/j.foodres.2013.12.009

Cheng, J.-H., & Sun, D.-W. (2015). Data fusion and hyperspectral imaging in tandem with least squares-support vector machine for prediction of sensory quality index scores of fish fillet. *Lebensmittel-Wissenschaft und -Technologie- Food Science and Technology, 63*(2), 892–898. https://doi.org/10.1016/j.lwt.2015.04.039

Cheng, W., Sun, D.-W., & Cheng, J.-H. (2016a). Pork biogenic amine index (Bai) determination based on chemometric analysis of hyperspectral imaging data. *Lebensmittel-Wissenschaft und -Technologie- Food Science and Technology, 73*, 13–19. https://doi.org/10.1016/j.lwt.2016.05.031

Cheng, W., Sun, D.-W., Pu, H., & Liu, Y. (2016b). Integration of spectral and textural data for enhancing hyperspectral prediction of K value in pork meat. *Lebensmittel-Wissenschaft und -Technologie- Food Science and Technology, 72*, 322–329. https://doi.org/10.1016/j.lwt.2016.05.003

Cheng, J.-H., Sun, D.-W., & Pu, H. (2016c). Combining the genetic algorithm and successive projection algorithm for the selection of feature wavelengths to evaluate exudative characteristics in frozen-thawed fish muscle. *Food Chemistry, 197*(Pt A), 855–863. https://doi.org/10.1016/j.foodchem.2015.11.019

Cheng, J.-H., Sun, D.-W., Pu, H.-B., Wang, Q.-J., & Chen, Y.-N. (2015a). Suitability of hyperspectral imaging for rapid evaluation of thiobarbituric acid (TBA) value in grass carp (*Ctenopharyngodon idella*) fillet. *Food Chemistry, 171*, 258–265. https://doi.org/10.1016/j.foodchem.2014.08.124

Cheng, J.-H., Sun, D.-W., Pu, H., & Zhu, Z. (2015b). Development of hyperspectral imaging coupled with chemometric analysis to monitor *K* value for evaluation of chemical spoilage in fish fillets. *Food Chemistry, 185*, 245–253. https://doi.org/10.1016/j.foodchem.2015.03.111

Cheng, J.-H., Sun, D.-W., & Wei, Q. (2017). Enhancing visible and near-infrared hyperspectral imaging prediction of TVB-N level for fish fillet freshness evaluation by filtering optimal variables. *Food Analytical Methods, 10*(6), 1888–1898. https://doi.org/10.1007/s12161-016-0742-9

Cheng, J.-H., Sun, D.-W., Pu, H., & Wei, Q. (2017b). Chemical spoilage extent traceability of two kinds of processed pork meats using one multispectral system developed by hyperspectral imaging combined with effective variable selection methods. *Food Chem, 221*, 1989–1996. https://doi.org/10.1016/j.foodchem.2016.11.093

Cheng, J.-H., Sun, D.-W., Pu, H., & Wei, Q. (2018). Heterospectral two-dimensional correlation analysis with near-infrared hyperspectral imaging for monitoring oxidative damage of pork myofibrils during frozen storage. *Food Chemistry, 248*, 119–127. https://doi.org/10.1016/j.foodchem.2017.12.050

Cheng, J.-H., Sun, D.-W., Zeng, X.-A., & Pu, H.-B. (2014b). Non-destructive and rapid determination of TVB-N content for freshness evaluation of grass carp (*Ctenopharyngodon idella*) by hyperspectral imaging. *Innovative Food Science & Emerging Technologies, 21*, 179–187. https://doi.org/10.1016/j.ifset.2013.10.013

Chen, J., & Rosenthal, A. (2015). Food texture and structure. In J. Chen, & A. Rosenthal (Eds.), *Novel ingredients and processing techniques: Vol. 1. Modifying food texture: Volume 1* (pp. 3–24). Oxford, UK: Woodhead Publishing. https://doi.org/10.1016/B978-1-78242-333-1.00001-2.

Chen, X., Zheng, L., & Kang, Z. (2020). Study on test method of kiwifruit hardness based on hyperspectral technique. *Journal of Physics: Conference Series, 1453*, Article 012143. https://doi.org/10.1088/1742-6596/1453/1/012143

Che, W., Sun, L., Zhang, Q., Tan, W., Ye, D., Zhang, D., & Liu, Y. (2018). Pixel based bruise region extraction of apple using Vis-NIR hyperspectral imaging. *Computers and Electronics in Agriculture, 146*, 12–21. https://doi.org/10.1016/j.compag.2018.01.013

Choi, N.-E., & Han, J. H. (2015). What is Taste?. *How flavor works: The science of taste and aroma*. UK: John Wiley & Sons. https://doi.org/10.1002/9781118865439.ch1

Cliff, M. A., & Toivonen, P. M. A. (2017). Sensory and quality characteristics of 'Ambrosia' apples in relation to harvest maturity for fruit stored up to eight months. *Postharvest Biology and Technology, 132*, 145–153. https://doi.org/10.1016/j.postharvbio.2017.05.015

Corbin, C. H., O'Quinn, T. G., Garmyn, A. J., Legako, J. F., Hunt, M. R., Dinh, T., Rathmann, R. J., Brooks, J. C., & Miller, M. F. (2015). Sensory evaluation of tender beef strip loin steaks of varying marbling levels and quality treatments. *Meat Science, 100*, 24–31. https://doi.org/10.1016/j.meatsci.2014.09.009

Dai, Q., Cheng, J.-H., Sun, D.-W., Pu, H., Zeng, X.-A., & Xiong, Z. (2015). Potential of visible/near-infrared hyperspectral imaging for rapid detection of freshness in unfrozen and frozen prawns. *Journal of Food Engineering, 149*, 97–104. https://doi.org/10.1016/j.jfoodeng.2014.10.001

Dai, Q., Cheng, J.-H., Sun, D.-W., & Zeng, X.-A. (2014). Potential of hyperspectral imaging for non-invasive determination of mechanical properties of prawn (*Metapenaeus ensis*). *Journal of Food Engineering, 136*, 64–72. https://doi.org/10.1016/j.jfoodeng.2014.03.013

Dai, Q., Cheng, J.-H., Sun, D.-W., Zhu, Z., & Pu, H. (2016). Prediction of total volatile basic nitrogen contents using wavelet features from visible/near-infrared hyperspectral images of prawn (Metapenaeus ensis). *Food Chemistry, 197*(Pt A), 257–265. https://doi.org/10.1016/j.foodchem.2015.10.073

De Huidobro, F. R., Miguel, E., Blázquez, B., & Onega, E. (2005). A comparison between two methods (Warner–Bratzler and texture profile analysis) for testing either raw meat or cooked meat. *Meat Science, 69*(3), 527–536. https://doi.org/10.1016/j.meatsci.2004.09.008

ElMasry, G., Barbin, D. F., Sun, D. W., & Allen, P. (2012). Meat quality evaluation by hyperspectral imaging technique: An overview. *Critical Reviews in Food Science and Nutrition, 52*(8), 689–711. https://doi.org/10.1080/10408398.2010.507908

ElMasry, G. M., & Nakauchi, S. (2016). Image analysis operations applied to hyperspectral images for non-invasive sensing of food quality–A comprehensive review. *Biosystems Engineering, 142*, 53–82. https://doi.org/10.1016/j.biosystemseng.2015.11.009

ElMasry, G., Sun, D.-W., & Allen, P. (2011). Non-destructive determination of water-holding capacity in fresh beef by using NIR hyperspectral imaging. *Food Research International, 44*(9), 2624–2633. https://doi.org/10.1016/j.foodres.2011.05.001

ElMasry, G., Sun, D.-W., & Allen, P. (2012). Near-infrared hyperspectral imaging for predicting colour, pH and tenderness of fresh beef. *Journal of Food Engineering, 110*(1), 127–140. https://doi.org/10.1016/j.jfoodeng.2011.11.028

Erkinbaev, C., Derksen, K., & Paliwal, J. (2019). Single kernel wheat hardness estimation using near infrared hyperspectral imaging. *Infrared Physics & Technology, 98*, 250–255. https://doi.org/10.1016/j.infrared.2019.03.033

Esquerre, C., Gowen, A. A., Downey, G., & O'Donnell, C. P. (2012). Wavelength selection for development of a near infrared imaging system for early detection of bruise damage in mushrooms (Agaricus bisporus). *Journal of Near Infrared Spectroscopy, 20*(5), 537–546. https://doi.org/10.1255/jnirs.1014

Fan, S., Huang, W., Guo, Z., Zhang, B., & Zhao, C. (2015). Prediction of soluble solids content and firmness of pears using hyperspectral reflectance imaging. *Food Analytical Methods, 8*(8), 1936–1946. https://doi.org/10.1007/s12161-014-0079-1

Fan, S., Li, C., Huang, W., & Chen, L. (2017). Detection of blueberry internal bruising over time using NIR hyperspectral reflectance imaging with optimum wavelengths. *Postharvest Biology and Technology, 134*, 55–66. https://doi.org/10.1016/j.postharvbio.2017.08.012

Feng, C.-H., & Makino, Y. (2020). Colour analysis in sausages stuffed in modified casings with different storage days using hyperspectral imaging–A feasibility study. *Food Control, 111*, Article 107047. https://doi.org/10.1016/j.foodcont.2019.107047

Feng, C.-H., Makino, Y., & García Martín, J. F. (2020). Hyperspectral imaging coupled with multivariate analysis and image processing for detection and visualisation of colour in cooked sausages stuffed in different modified casings. *Foods, 9*(8), 1089. https://doi.org/10.3390/foods9081089

Feng, C.-H., Makino, Y., Yoshimura, M., & Rodríguez-Pulido, F. J. (2017). Real-time prediction of pre-cooked Japanese sausage color with different storage days using hyperspectral imaging. *Journal of the Science of Food and Agriculture, 98*(7), 2564–2572. https://doi.org/10.1002/jsfa.8746

Feng, L., Zhu, S., Zhou, L., Zhao, Y., Bao, Y., Zhang, C., & He, Y. (2019). Detection of subtle bruises on winter jujube using hyperspectral imaging with pixel-wise deep learning method. *IEEE Access, 7*, 64494–64505. https://doi.org/10.1109/ACCESS.2019.2917267

Ferrari, C., Foca, G., Calvini, R., & Ulrici, A. (2015). Fast exploration and classification of large hyperspectral image datasets for early bruise detection on apples. *Chemometrics and Intelligent Laboratory Systems, 146*, 108–119. https://doi.org/10.1016/j.chemolab.2015.05.016

Feuz, D. M., Umberger, W. J., Calkins, C. R., & Sitz, B. (2004). US consumers' willingness to pay for flavor and tenderness in steaks as determined with an experimental auction. *Journal of Agricultural and Resource Economics, 501–516*. Retrieved October 3, 2020, from http://www.jstor.org/stable/40987246.

Fischer, K. (2007). Drip loss in pork: Influencing factors and relation to further meat quality traits. *Journal of Animal Breeding and Genetics, 124*, 12–18. https://doi.org/10.1111/j.1439-0388.2007.00682.x

Gao, Z., Shao, Y., Xuan, G., Wang, Y., Liu, Y., & Han, X. (2020). Real-time hyperspectral imaging for the in-field estimation of strawberry ripeness with deep learning. *Artificial Intelligence in Agriculture, 4*, 31–38. https://doi.org/10.1016/j.aiia.2020.04.003

He, H.-J., Wu, D., & Sun, D.-W. (2014a). Potential of hyperspectral imaging combined with chemometric analysis for assessing and visualising tenderness distribution in raw farmed salmon fillets. *Journal of Food Engineering, 126*, 156–164. https://doi.org/10.1016/j.jfoodeng.2013.11.015

He, H.-J., Wu, D., & Sun, D.-W. (2014b). Rapid and non-destructive determination of drip loss and pH distribution in farmed Atlantic salmon (*Salmo salar*) fillets using visible and near-infrared (Vis-NIR) hyperspectral imaging. *Food Chemistry, 156*, 394–401. https://doi.org/10.1016/j.foodchem.2014.01.118

Howgate, P. (2015). A history of the development of sensory methods for the evaluation of freshness of fish. *Journal of Aquatic Food Product Technology, 24*(5), 516–532. https://doi.org/10.1080/10498850.2013.783897

Huang, M., Wang, Q., Zhang, M., & Zhu, Q. (2014). Prediction of color and moisture content for vegetable soybean during drying using hyperspectral imaging technology. *Journal of Food Engineering, 128*, 24–30. https://doi.org/10.1016/j.jfoodeng.2013.12.008

Hu, M.-H., Dong, Q.-L., Liu, B.-L., Opara, U. L., & Chen, L. (2015). Estimating blueberry mechanical properties based on random frog selected hyperspectral data. *Postharvest Biology and Technology, 106*, 1–10. https://doi.org/10.1016/j.postharvbio.2015.03.014

Iqbal, A., Sun, D.-W., & Allen, P. (2013). Prediction of moisture, color and pH in cooked, pre-sliced Turkey hams by NIR hyperspectral imaging system. *Journal of Food Engineering, 117*(1), 42–51. https://doi.org/10.1016/j.jfoodeng.2013.02.001

Ivorra, E., Verdu, S., Sánchez, A. J., Grau, R., & Barat, J. M. (2016). Predicting gilthead sea bream (*Sparus aurata*) freshness by a novel combined technique of 3D imaging and SW-NIR spectral analysis. *Sensors, 16*(10), 1735. https://doi.org/10.3390/s16101735

Jara-Palacios, M. J., Rodríguez-Pulido, F. J., Hernanz, D., Escudero-Gilete, M. L., & Heredia, F. J. (2016). Determination of phenolic substances of seeds, skins and stems from white grape marc by near-infrared hyperspectral imaging. *Australian Journal of Grape and Wine Research, 22*(1), 11–15. https://doi.org/10.1111/ajgw.12165

Jiang, H., Yoon, S.-C., Zhuang, H., Wang, W., Li, Y., Lu, C., & Li, N. (2018). Non-destructive assessment of final color and pH attributes of broiler breast fillets using visible and near-infrared hyperspectral imaging: A preliminary study. *Infrared Physics & Technology, 92*, 309–317. https://doi.org/10.1016/j.infrared.2018.06.025

Ji, Y., Sun, L., Li, Y., & Ye, D. (2019). Detection of bruised potatoes using hyperspectral imaging technique based on discrete wavelet transform. *Infrared Physics & Technology, 103*, 103054. https://doi.org/10.1016/j.infrared.2019.103054

Kamruzzaman, M., ElMasry, G., Sun, D.-W., & Allen, P. (2012). Prediction of some quality attributes of lamb meat using near-infrared hyperspectral imaging and multivariate analysis. *Analytica Chimica Acta, 714*, 57–67. https://doi.org/10.1016/j.aca.2011.11.037

Kamruzzaman, M., ElMasry, G., Sun, D.-W., & Allen, P. (2013). Non-destructive assessment of instrumental and sensory tenderness of lamb meat using NIR hyperspectral imaging. *Food Chemistry, 141*(1), 389–396. https://doi.org/10.1016/j.foodchem.2013.02.094

Kamruzzaman, M., Sun, D.-W., ElMasry, G., & Allen, P. (2013). Fast detection and visualization of minced lamb meat adulteration using NIR hyperspectral imaging and multivariate image analysis. *Talanta, 103*, 130–136. https://doi.org/10.1016/j.talanta.2012.10.020

Kamruzzaman, M., Makino, Y., & Oshita, S. (2016a). Hyperspectral imaging for real-time monitoring of water holding capacity in red meat. *LWT-Food Science and Technology, 66*, 685–691. https://doi.org/10.1016/j.lwt.2015.11.021

Kamruzzaman, M., Makino, Y., & Oshita, S. (2016b). Online monitoring of red meat color using hyperspectral imaging. *Meat Science, 116*, 110–117. https://doi.org/10.1016/j.meatsci.2016.02.004

Keresztes, J. C., Goodarzi, M., & Saeys, W. (2016). Real-time pixel based early apple bruise detection using short wave infrared hyperspectral imaging in combination with calibration and glare correction techniques. *Food Control, 66*, 215–226. https://doi.org/10.1016/j.foodcont.2016.02.007

Lawless, H. T., & Heymann, H. (2013). *Sensory evaluation of food: Principles and practices*. New York: Springer Science & Business Media. https://doi.org/10.1007/978-1-4615-7843-7

Lee, W.-H., Kim, M. S., Lee, H., Delwiche, S. R., Bae, H., Kim, D.-Y., & Cho, B.-K. (2014). Hyperspectral near-infrared imaging for the detection of physical damages of pear. *Journal of Food Engineering, 130*, 1–7. https://doi.org/10.1016/j.jfoodeng.2013.12.032

Lei, T., & Sun, D.-W. (2019). Developments of nondestructive techniques for evaluating quality attributes of cheeses: A review. *Trends in Food Science & Technology, 88*, 527–542. https://doi.org/10.1016/j.tifs.2019.04.013

Leiva-Valenzuela, G. A., Lu, R., & Aguilera, J. M. (2013). Prediction of firmness and soluble solids content of blueberries using hyperspectral reflectance imaging. *Journal of Food Engineering, 115*(1), 91–98. https://doi.org/10.1016/j.jfoodeng.2012.10.001

Li, J., Chen, L., & Huang, W. (2018a). Detection of early bruises on peaches (*Amygdalus persica* L.) using hyperspectral imaging coupled with improved watershed segmentation algorithm. *Postharvest Biology and Technology, 135*, 104–113. https://doi.org/10.1016/j.postharvbio.2017.09.007

Li, H., Chen, Q., Zhao, J., & Wu, M. (2015). Nondestructive detection of total volatile basic nitrogen (TVB-N) content in pork meat by integrating hyperspectral imaging and colorimetric sensor combined with a nonlinear data fusion. *LWT-Food Science and Technology, 63*(1), 268–274. https://doi.org/10.1016/j.lwt.2015.03.052

Li, B., Cobo-Medina, M., Lecourt, J., Harrison, N., Harrison, R. J., & Cross, J. V. (2018b). Application of hyperspectral imaging for nondestructive measurement of plum quality attributes. *Postharvest Biology and Technology, 141*, 8–15. https://doi.org/10.1016/j.postharvbio.2018.03.008

Lin, X., & Sun, D.-W. (2020). Recent developments in vibrational spectroscopic techniques for tea quality and safety analyses. *Trends in Food Science & Technology, 104*, 163–176. https://doi.org/10.1016/j.tifs.2020.06.009

Li, Y., Shan, J., Peng, Y., & Gao, X. (2011). Nondestructive assessment of beef-marbling grade using hyperspectral imaging technology. In *2011 international conference on new technology of agricultural* (pp. 779–783). https://doi.org/10.1109/ICAE.2011.5943908

Liu, J., Liu, S., Shin, S., Liu, F., Shi, T., Lv, C., & Men, H. (2020). Detection of apple taste information using model based on hyperspectral imaging and electronic tongue data. *Sensors and Materials, 32*(5), 1767–1784. https://doi.org/10.18494/SAM.2020.2715

Liu, D., Ma, J., Sun, D.-W., Pu, H., Gao, W., Qu, J., & Zeng, X.-A. (2014). Prediction of color and pH of salted porcine meats using visible and near-infrared hyperspectral imaging. *Food and Bioprocess Technology, 7*(11), 3100–3108. https://doi.org/10.1007/s11947-014-1327-5

Liu, L., & Ngadi, M. O. (2014). Predicting intramuscular fat content of pork using hyperspectral imaging. *Journal of Food Engineering, 134*, 16–23. https://doi.org/10.1016/j.jfoodeng.2014.02.007

Liu, Y., Pu, H., & Sun, D.-W. (2017). Hyperspectral imaging technique for evaluating food quality and safety during various processes: A review of recent applications. *Trends in Food Science & Technology, 69*, 25–35. https://doi.org/10.1016/j.tifs.2017.08.013

Liu, Y., Sun, D.-W., Cheng, J.-H., & Han, Z. (2018). Hyperspectral imaging sensing of changes in moisture content and color of beef during microwave heating process. *Food Analytical Methods, 11*(9), 2472–2484. https://doi.org/10.1007/s12161-018-1234-x

Li, X., Wei, Y., Xu, J., Feng, X., Wu, F., Zhou, R., Jin, J., Xu, K., Yu, X., & He, Y. (2018c). SSC and pH for sweet assessment and maturity classification of harvested cherry fruit based on NIR hyperspectral imaging technology. *Postharvest Biology and Technology, 143*, 112–118. https://doi.org/10.1016/j.postharvbio.2018.05.003

Lu, R., & Cen, H. (2013). Non-destructive methods for food texture assessment. In *Instrumental assessment of food sensory quality: A practical guide* (pp. 230–255e). Cambridge, UK: Woodhead Publishing.

Lurie, S., & Crisosto, C. H. (2005). Chilling injury in peach and nectarine. *Postharvest Biology and Technology, 37*(3), 195–208. https://doi.org/10.1016/j.postharvbio.2005.04.012

Lü, Q., Tang, M.-J., Cai, J.-R., Zhao, J.-W., & Vittayapadung, S. (2011). Vis/NIR hyperspectral imaging for detection of hidden bruises on kiwifruits. *Czech Journal of Food Sciences, 29*(6), 595–602. https://doi.org/10.17221/69/2010-CJFS

Lu, H., Yu, X., Zhou, L., & He, Y. (2018). Selection of spectral resolution and scanning speed for detecting green jujubes chilling injury based on hyperspectral reflectance imaging. *Applied Sciences, 8*(4), 523. https://doi.org/10.3390/app8040523

MacDougall, D. B. (2010). Colour measurement of food: Principles and practice. In *Colour measurement: Principles, advances and industrial applications* (pp. 312–342). UK: Woodhead Publishing. https://doi.org/10.1533/9780857090195.2.312.

Ma, J., Sun, D.-W., & Pu, H. (2017). Model improvement for predicting moisture content (MC) in pork longissimus dorsi muscles under diverse processing conditions by hyperspectral imaging. *Journal of Food Engineering, 196*, 65–72. https://doi.org/10.1016/j.jfoodeng.2016.10.016

Ma, J., Sun, D.-W., Pu, H., Cheng, J.-H., & Wei, Q. (2019). Advanced techniques for hyperspectral imaging in the food industry: Principles and recent applications. *Annual Review of Food Science and Technology, 10*, 197–220. https://doi.org/10.1146/annurev-food-032818-121155

Ma, J., Sun, D.-W., Qu, J.-H., & Pu, H. (2017). Prediction of textural changes in grass carp fillets as affected by vacuum freeze drying using hyperspectral imaging based on integrated group wavelengths. *LWT-Food Science and Technology, 82*, 377–385. https://doi.org/10.1016/j.lwt.2017.04.040

Ma, J., Pu, H., & Sun, D.-W. (2018). Predicting intramuscular fat content variations in boiled pork muscles by hyperspectral imaging using a novel spectral pre-processing technique. *LWT, 94*, 119–128. https://doi.org/10.1016/j.lwt.2018.04.030

Mendoza, F. A., Cichy, K. A., Sprague, C., Goffnett, A., Lu, R., & Kelly, J. D. (2018). Prediction of canned black bean texture (*Phaseolus vulgaris* L.) from intact dry seeds using visible/near infrared spectroscopy and hyperspectral imaging data. *Journal of the Science of Food and Agriculture, 98*(1), 283–290. https://doi.org/10.1002/jsfa.8469

Mendoza, F., Lu, R., Ariana, D., Cen, H., & Bailey, B. (2011). Integrated spectral and image analysis of hyperspectral scattering data for prediction of apple fruit firmness and soluble solids content. *Postharvest Biology and Technology, 62*(2), 149–160. https://doi.org/10.1016/j.postharvbio.2011.05.009

Miller, R. K. (2014). Chemical and physical characteristics of meat/palatability. In M. Dikeman, & C. Devine (Eds.), *Encyclopedia of meat sciences* (2nd ed., pp. 252–261). Oxford: Academic Press.

Mohammadi-Moghaddam, T., Razavi, S. M., Taghizadeh, M., Pradhan, B., Sazgarnia, A., & Shaker-Ardekani, A. (2018). Hyperspectral imaging as an effective tool for prediction the moisture content and textural characteristics of roasted pistachio kernels. *Journal of Food Measurement and Characterization, 12*(3), 1493–1502. https://doi.org/10.1007/s11694-018-9764-x

Munera, S., Aleixos, N., Besada, C., Gómez-Sanchis, J., Salvador, A., Cubero, S., & Blasco, J. (2019a). Discrimination of astringent and deastringed hard 'Rojo Brillante'persimmon fruit using a sensory threshold by means of hyperspectral imaging. *Journal of Food Engineering, 263*, 173–180. https://doi.org/10.1016/j.jfoodeng.2019.06.008

Munera, S., Amigo, J. M., Blasco, J., Cubero, S., Talens, P., & Aleixos, N. (2017a). Ripeness monitoring of two cultivars of nectarine using VIS-NIR hyperspectral reflectance imaging. *Journal of Food Engineering, 214*, 29–39. https://doi.org/10.1016/j.jfoodeng.2017.06.031

Munera, S., Besada, C., Aleixos, N., Talens, P., Salvador, A., Sun, D.-W., Cubero, S., & Blasco, J. (2017b). Non-destructive assessment of the internal quality of intact persimmon using colour and VIS/NIR hyperspectral imaging. *LWT-Food Science and Technology, 77*, 241–248. https://doi.org/10.1016/j.lwt.2016.11.063

Munera, S., Besada, C., Blasco, J., Cubero, S., Salvador, A., Talens, P., & Aleixos, N. (2017c). Astringency assessment of persimmon by hyperspectral imaging. *Postharvest Biology and Technology, 125*, 35–41. https://doi.org/10.1016/j.postharvbio.2016.11.006

Munera, S., Hernández, F., Aleixos, N., Cubero, S., & Blasco, J. (2019b). Maturity monitoring of intact fruit and arils of pomegranate cv. 'Mollar de Elche' using machine vision and chemometrics. *Postharvest Biology and Technology, 156*, Article 110936. https://doi.org/10.1016/j.postharvbio.2019.110936

Murray, J. M., Delahunty, C. M., & Baxter, I. A. (2001). Descriptive sensory analysis: Past, present and future. *Food Research International, 34*(6), 461–471. https://doi.org/10.1016/S0963-9969(01)00070-9

Nguyen-Do-Trong, N., Dusabumuremyi, J. C., & Saeys, W. (2018). Cross-polarized VNIR hyperspectral reflectance imaging for non-destructive quality evaluation of dried banana slices, drying process monitoring and control. *Journal of Food Engineering, 238*, 85–94. https://doi.org/10.1016/j.jfoodeng.2018.06.013

Nogales-Bueno, J., Rodríguez-Pulido, F. J., Heredia, F. J., & Hernández-Hierro, J. M. (2015). Comparative study on the use of anthocyanin profile, color image analysis and near-infrared hyperspectral imaging as tools to discriminate between four autochthonous red grape cultivars from La Rioja (Spain). *Talanta, 131*, 412–416. https://doi.org/10.1016/j.talanta.2014.07.086

Pan, Y., Sun, D.-W., Cheng, J.-H., & Han, Z. (2018). Non-destructive detection and screening of non-uniformity in microwave sterilization using hyperspectral imaging analysis. *Food Analytical Methods, 11*(6), 1568–1580. https://doi.org/10.1007/s12161-017-1134-5

Pan, L., Zhang, Q., Zhang, W., Sun, Y., Hu, P., & Tu, K. (2016). Detection of cold injury in peaches by hyperspectral reflectance imaging and artificial neural network. *Food Chemistry, 192*, 134–141. https://doi.org/10.1016/j.foodchem.2015.06.106

Pathare, P. B., Opara, U. L., & Al-Said, F. A. J. (2013). Colour measurement and analysis in fresh and processed foods: A review. *Food and Bioprocess Technology, 6*(1), 36–60. https://doi.org/10.1007/s11947-012-0867-9

Péneau, S., Hoehn, E., Roth, H. R., Escher, F., & Nuessli, J. (2006). Importance and consumer perception of freshness of apples. *Food Quality and Preference, 17*(1–2), 9–19. https://doi.org/10.1016/j.foodqual.2005.05.002

Priyashantha, H., Höjer, A., Saedén, K. H., Lundh, Å., Johansson, M., Bernes, G., & Hetta, M. (2020). Use of near-infrared hyperspectral (NIR-HS) imaging to visualize and model the maturity of long-ripening hard cheeses. *Journal of Food Engineering, 264*, 109687. https://doi.org/10.1016/j.jfoodeng.2019.109687

Pu, H., Liu, D., Wang, L., & Sun, D.-W. (2016). Soluble solids content and pH prediction and maturity discrimination of lychee fruits using visible and near infrared hyperspectral imaging. *Food Analytical Methods, 9*(1), 235–244. https://doi.org/10.1007/s12161-015-0186-7

Purchas, R. W. (2014). Tenderness measurement. In M. Dikeman, & C. Devine (Eds.), *Encyclopedia of meat sciences* (2nd ed., pp. 452–459). Oxford: Academic Press.

Pu, Y.-Y., Sun, D.-W., Buccheri, M., Grassi, M., Cattaneo, T. M., & Gowen, A. (2019). Ripeness classification of bananito fruit (*Musa acuminata*, AA): A comparison study of visible spectroscopy and hyperspectral imaging. *Food Analytical Methods, 12*(8), 1693–1704. https://doi.org/10.1007/s12161-019-01506-7

Rahman, A., Faqeerzada, M. A., & Cho, B. K. (2018a). Hyperspectral imaging for predicting the allicin and soluble solid content of garlic with variable selection algorithms and chemometric models. *Journal of the Science of Food and Agriculture, 98*(12), 4715–4725. https://doi.org/10.1002/jsfa.9006

Rahman, A., Lee, H., Kim, M. S., & Cho, B.-K. (2018b). Mapping the pungency of green pepper using hyperspectral imaging. *Food Analytical Methods, 11*(11), 3042–3052. https://doi.org/10.1007/s12161-018-1275-1

Rahman, A., Park, E., Bae, H., & Cho, B.-K. (2018c). Hyperspectral imaging technique to evaluate the firmness and the sweetness index of tomatoes. *Korean Journal of Animal Science, 45*(4), 823–837. https://doi.org/10.7744/kjoas.20180075

Rajkumar, P., Wang, N., EImasry, G., Raghavan, G. S. V., & Gariepy, Y. (2012). Studies on banana fruit quality and maturity stages using hyperspectral imaging. *Journal of Food Engineering, 108*(1), 194–200. https://doi.org/10.1016/j.jfoodeng.2011.05.002

Reddy, R. P., & Li, M. (2020). Uncertainty assessment for firmness and total soluble solids of sweet cherries using hyperspectral imaging and multivariate statistics. *Journal of Food Engineering*, 110177. https://doi.org/10.1016/j.jfoodeng.2020.110177

Rodríguez-Pulido, F. J., Hernández-Hierro, J. M., Nogales-Bueno, J., Gordillo, B., González-Miret, M. L., & Heredia, F. J. (2014). A novel method for evaluating flavanols in grape seeds by near infrared hyperspectral imaging. *Talanta, 122*, 145–150. https://doi.org/10.1016/j.talanta.2014.01.044

Roque, J., Auvray, M., & Lafraire, J. (2018). Understanding freshness perception from the cognitive mechanisms of flavor: The case of beverages. *Frontiers in Psychology, 8*, 2360. https://doi.org/10.3389/fpsyg.2017.02360

Roy, J.v, Keresztes, J. C., Wouters, N., De Ketelaere, B., & Saeys, W. (2017). Measuring colour of vine tomatoes using hyperspectral imaging. *Postharvest Biology and Technology, 129*, 79–89. https://doi.org/10.1016/j.postharvbio.2017.03.006

Rungpichayapichet, P., Nagle, M., Yuwanbun, P., Khuwijitjaru, P., Mahayothee, B., & Müller, J. (2017). Prediction mapping of physicochemical properties in mango by hyperspectral imaging. *Biosystems Engineering, 159*, 109–120. https://doi.org/10.1016/j.biosystemseng.2017.04.006

Song, H., & Liu, J. (2018). GC-O-MS technique and its applications in food flavor analysis. *Food Research International, 114*, 187–198. https://doi.org/10.1016/j.foodres.2018.07.037

Suktanarak, S., & Teerachaichayut, S. (2017). Non-destructive quality assessment of hens' eggs using hyperspectral images. *Journal of Food Engineering, 215*, 97–103. https://doi.org/10.1016/j.jfoodeng.2017.07.008

Sun, D.-W. (Ed.). (2010). *Hyperspectral imaging for food quality analysis and control*. UK: Elsevier.

Sun, Y., Gu, X., Sun, K., Hu, H., Xu, M., Wang, Z., Tu, K., & Pan, L. (2017a). Hyperspectral reflectance imaging combined with chemometrics and successive projections algorithm for chilling injury classification in peaches. *LWT-Food Science and Technology, 75*, 557–564. https://doi.org/10.1016/j.lwt.2016.10.006

Sun, M., Zhang, D., Liu, L., & Wang, Z. (2017b). How to predict the sugariness and hardness of melons: A near-infrared hyperspectral imaging method. *Food Chemistry, 218*, 413–421. https://doi.org/10.1016/j.foodchem.2016.09.023

Su, W.-H., & Sun, D.-W. (2018). Fourier transform infrared and Raman and hyperspectral imaging techniques for quality determinations of powdery foods: A review. *Comprehensive Reviews in Food Science and Food Safety, 17*(1), 104–122. https://doi.org/10.1111/1541-4337.12314

Szczesniak, A. S. (2002). Texture is a sensory property. *Food Quality and Preference, 13*(4), 215–225. https://doi.org/10.1016/S0950-3293(01)00039-8

Tan, W., Sun, L., Yang, F., Che, W., Ye, D., Zhang, D., & Zou, B. (2018). Study on bruising degree classification of apples using hyperspectral imaging and GS-SVM. *Optik, 154*, 581–592. https://doi.org/10.1016/j.ijleo.2017.10.090

Tao, F., Peng, Y., Li, Y., Chao, K., & Dhakal, S. (2012). Simultaneous determination of tenderness and Escherichia coli contamination of pork using hyperspectral scattering technique. *Meat Science, 90*(3), 851–857. https://doi.org/10.1016/j.meatsci.2011.11.028

Teerachaichayut, S., & Ho, H. T. (2017). Non-destructive prediction of total soluble solids, titratable acidity and maturity index of limes by near infrared hyperspectral imaging. *Postharvest Biology and Technology, 133*, 20–25. https://doi.org/10.1016/j.postharvbio.2017.07.005

Thompson, J. M. (2004). The effects of marbling on flavour and juiciness scores of cooked beef, after adjusting to a constant tenderness. *Australian Journal of Experimental Agriculture, 44*(7), 645–652. https://doi.org/10.1071/EA02171

Tschannerl, J., Ren, J., Jack, F., Krause, J., Zhao, H., Huang, W., & Marshall, S. (2019). Potential of UV and SWIR hyperspectral imaging for determination of levels of phenolic flavour compounds in peated barley malt. *Food Chemistry, 270*, 105–112. https://doi.org/10.1016/j.foodchem.2018.07.089

Tu, Y., Bian, M., Wan, Y., & Fei, T. (2018). Tea cultivar classification and biochemical parameter estimation from hyperspectral imagery obtained by UAV. *PeerJ, 6*, Article e4858. https://doi.org/10.7717/peerj.4858

Velásquez, L., Cruz-Tirado, J. P., Siche, R., & Quevedo, R. (2017). An application based on the decision tree to classify the marbling of beef by hyperspectral imaging. *Meat Science, 133*, 43–50. https://doi.org/10.1016/j.meatsci.2017.06.002

Wang, M., Gao, F., Wu, Q., Zhang, J., Xue, Y., Wan, H., & Wang, P. (2018). Real-time assessment of food freshness in refrigerators based on a miniaturized electronic nose. *Analytical Methods, 10*(39), 4741–4749. https://doi.org/10.1039/C8AY01242C

Wang, S., Huang, M., & Zhu, Q. (2012). Model fusion for prediction of apple firmness using hyperspectral scattering image. *Computers and Electronics in Agriculture, 80*, 1–7. https://doi.org/10.1016/j.compag.2011.10.008

Wang, L., Pu, H., Sun, D.-W., Liu, D., Wang, Q., & Xiong, Z. (2015). Application of hyperspectral imaging for prediction of textural properties of maize seeds with different storage periods. *Food Analytical Methods, 8*(6), 1535–1545. https://doi.org/10.1007/s12161-014-0029-y

Wang, X., Russel, M., Zhang, Y., Zhao, J., Zhang, Y., & Shan, J. (2019a). A clustering-based partial least squares method for improving the freshness prediction model of crucian carps fillets by hyperspectral image technology. *Food Analytical Methods, 12*(9), 1988–1997. https://doi.org/10.1007/s12161-019-01541-4

Wang, X., Shan, J., Han, S., Zhao, J., & Zhang, Y. (2019b). Optimization of fish quality by evaluation of total volatile basic nitrogen (TVB-N) and texture profile analysis (TPA) by near-infrared (NIR) hyperspectral imaging. *Analytical Letters, 52*(12), 1845–1859. https://doi.org/10.1080/00032719.2019.1571077

Wang, N.-N., Sun, D.-W., Yang, Y.-C., Pu, H., & Zhu, Z. (2016). Recent advances in the application of hyperspectral imaging for evaluating fruit quality. *Food Analytical Methods, 9*(1), 178–191. https://doi.org/10.1007/s12161-015-0153-3

Wei, X., He, J.-C., Ye, D.-P., & Jie, D.-F. (2017). Navel orange maturity classification by multispectral indexes based on hyperspectral diffuse transmittance imaging. *Journal of Food Quality*, 1–7. https://doi.org/10.1155/2017/1023498, 2017.

Wei, X., Liu, F., Qiu, Z., Shao, Y., & He, Y. (2014). Ripeness classification of astringent persimmon using hyperspectral imaging technique. *Food and Bioprocess Technology, 7*(5), 1371–1380. https://doi.org/10.1007/s11947-013-1164-y

Wu, J., Peng, Y., Li, Y., Wang, W., Chen, J., & Dhakal, S. (2012a). Prediction of beef quality attributes using VIS/NIR hyperspectral scattering imaging technique. *Journal of Food Engineering, 109*(2), 267–273. https://doi.org/10.1016/j.jfoodeng.2011.10.004

Wu, D., & Sun, D.-W. (2013a). Advanced applications of hyperspectral imaging technology for food quality and safety analysis and assessment: A review—Part I: Fundamentals. *Innovative Food Science & Emerging Technologies, 19*, 1–14. https://doi.org/10.1016/j.ifset.2013.04.014

Wu, D., & Sun, D.-W. (2013b). Advanced applications of hyperspectral imaging technology for food quality and safety analysis and assessment: A review—Part II: Applications. *Innovative Food Science & Emerging Technologies, 19*, 15–28. https://doi.org/10.1016/j.ifset.2013.04.016

Wu, D., Sun, D.-W., & He, Y. (2012b). Application of long-wave near infrared hyperspectral imaging for measurement of color distribution in salmon fillet. *Innovative Food Science & Emerging Technologies, 16*, 361–372. https://doi.org/10.1016/j.ifset.2012.08.003

Wu, D., Sun, D.-W., & He, Y. (2014). Novel non-invasive distribution measurement of texture profile analysis (TPA) in salmon fillet by using visible and near infrared hyperspectral imaging. *Food Chemistry, 145*, 417–426. https://doi.org/10.1016/j.foodchem.2013.08.063

Wu, J., & Yu, Y. (2015). Prediction of fresh pork quality using hyperspectral scattering imaging (HSI) technique. *Animal Husbandry and Feed Science, 7*(3), 144.

Xiao, Q., Bai, X., & He, Y. (2020). Rapid screen of the color and water content of fresh-cut potato tuber slices using hyperspectral imaging coupled with multivariate analysis. *Foods, 9*(1), 94. https://doi.org/10.3390/foods9010094

Xie, C., Chu, B., & He, Y. (2018). Prediction of banana color and firmness using a novel wavelengths selection method of hyperspectral imaging. *Food Chemistry, 245*, 132–140. https://doi.org/10.1016/j.foodchem.2017.10.079

Xie, C., Li, X., Shao, Y., & He, Y. (2014). Color measurement of tea leaves at different drying periods using hyperspectral imaging technique. *PloS One, 9*(12), Article e113422. https://doi.org/10.1371/journal.pone.0113422

Xie, A., Sun, D.-W., Xu, Z., & Zhu, Z. (2015). Rapid detection of frozen pork quality without thawing by Vis–NIR hyperspectral imaging technique. *Talanta, 139*, 208–215. https://doi.org/10.1016/j.talanta.2015.02.027

Xiong, Z., Sun, D.-W., Dai, Q., Han, Z., Zeng, X.-A., & Wang, L. (2015a). Application of visible hyperspectral imaging for prediction of springiness of fresh chicken meat. *Food Analytical Methods, 8*(2), 380–391. https://doi.org/10.1007/s12161-014-9853-3

Xiong, Z., Sun, D.-W., Pu, H., Xie, A., Han, Z., & Luo, M. (2015b). Non-destructive prediction of thiobarbituric acid reactive substances (TBARS) value for freshness evaluation of chicken meat using hyperspectral imaging. *Food Chemistry, 179*, 175–181. https://doi.org/10.1016/j.foodchem.2015.01.116

Xiong, Z., Sun, D.-W., Zeng, X.-A., & Xie, A. (2014). Recent developments of hyperspectral imaging systems and their applications in detecting quality attributes of red meats: A review. *Journal of Food Engineering, 132*, 1–13. https://doi.org/10.1016/j.jfoodeng.2014.02.004

Yang, C., Lee, W. S., & Gader, P. (2014). Hyperspectral band selection for detecting different blueberry fruit maturity stages. *Computers and Electronics in Agriculture, 109*, 23–31. https://doi.org/10.1016/j.compag.2014.08.009

Yang, Q., Sun, D.-W., & Cheng, W. (2017). Development of simplified models for nondestructive hyperspectral imaging monitoring of TVB-N contents in cured meat during drying process. *Journal of Food Engineering, 192*, 53–60. https://doi.org/10.1016/j.jfoodeng.2016.07.015

Yang, Y., Wang, W., Zhuang, H., Yoon, S.-C., & Jiang, H. (2018). Fusion of spectra and texture data of hyperspectral imaging for the prediction of the water-holding capacity of fresh chicken breast filets. *Applied Sciences, 8*(4), 640. https://doi.org/10.3390/app8040640

Yao, K., Sun, J., Zhou, X., Nirere, A., Tian, Y., & Wu, X. (2020). Nondestructive detection for egg freshness grade based on hyperspectral imaging technology. *Journal of Food Process Engineering*. , Article e13422. https://doi.org/10.1111/jfpe.13422

Ye, R., Chen, Y., Guo, Y., Duan, Q., Li, D., & Liu, C. (2020). NIR hyperspectral imaging technology combined with multivariate methods to identify shrimp freshness. *Applied Sciences, 10*(16), 5498. https://doi.org/10.3390/app10165498

Ye, D., Sun, L., Tan, W., Che, W., & Yang, M. (2018). Detecting and classifying minor bruised potato based on hyperspectral imaging. *Chemometrics and Intelligent Laboratory Systems, 177*, 129–139. https://doi.org/10.1016/j.chemolab.2018.04.002

Yu, D., Xu, T., & Song, K. (2020). Identification of Nanguo pear maturity based on information fusion. *Journal of Applied Spectroscopy*. https://doi.org/10.1007/s10812-020-01008-z

Zhang, H., Gu, B., Mu, J., Ruan, P., & Li, D. (2017). Wheat hardness prediction research based on NIR hyperspectral analysis combined with ant colony optimization algorithm. *Procedia Engineering, 174*, 648–656. https://doi.org/10.1016/j.proeng.2017.01.202

Zhang, C., Guo, C., Liu, F., Kong, W., He, Y., & Lou, B. (2016). Hyperspectral imaging analysis for ripeness evaluation of strawberry with support vector machine. *Journal of Food Engineering, 179*, 11–18. https://doi.org/10.1016/j.jfoodeng.2016.01.002

Zhang, M., Jiang, Y., Li, C., & Yang, F. (2020). Fully convolutional networks for blueberry bruising and calyx segmentation using hyperspectral transmittance imaging. *Biosystems Engineering, 192*, 159–175. https://doi.org/10.1016/j.biosystemseng.2020.01.018

Zhang, W., Pan, L., Tu, S., Zhan, G., & Tu, K. (2015). Non-destructive internal quality assessment of eggs using a synthesis of hyperspectral imaging and multivariate analysis. *Journal of Food Engineering, 157*, 41–48. https://doi.org/10.1016/j.jfoodeng.2015.02.013

Zhu, H., Chu, B., Fan, Y., Tao, X., Yin, W., & He, Y. (2017). Hyperspectral imaging for predicting the internal quality of kiwifruits based on variable selection algorithms and chemometric models. *Scientific Reports, 7*(1), 1–13. https://doi.org/10.1038/s41598-017-08509-6

Zhu, S., Feng, L., Zhang, C., Bao, Y., & He, Y. (2019). Identifying freshness of spinach leaves stored at different temperatures using hyperspectral imaging. *Foods, 8*(9), 356. https://doi.org/10.3390/foods8090356

Zhu, Q., He, C., Lu, R., Mendoza, F., & Cen, H. (2015). Ripeness evaluation of 'Sun Bright' tomato using optical absorption and scattering properties. *Postharvest Biology and Technology, 103*, 27–34. https://doi.org/10.1016/j.postharvbio.2015.02.007

Zhu, Q., Huang, M., Zhao, X., & Wang, S. (2013). Wavelength selection of hyperspectral scattering image using new semi-supervised affinity propagation for prediction of firmness and soluble solid content in apples. *Food Analytical Methods, 6*(1), 334–342. https://doi.org/10.1007/s12161-012-9442-2

Zou, S., Tseng, Y. C., Zare, A., Rowland, D. L., Tillman, B. L., & Yoon, S. C. (2019). Peanut maturity classification using hyperspectral imagery. *Biosystems Engineering, 188*, 165–177. https://doi.org/10.1016/j.biosystemseng.2019.10.019